의학박사 학위논문

Comprehensive immune profiling and analysis of significance of S100A8-positive immune cells in breast cancer

유방암 조직의 포괄적인 면역 프로파일링과 S100A8 양성 면역세포의 의의 분석

February 2022

서울대학교 대학원
의학과 병리학전공
우 지 원

Comprehensive immune profiling and analysis of significance of S100A8-positive immune cells in breast cancer

October 2021

Graduate School of Medicine
Seoul National University
Pathology Major

Ji Won Woo

Confirming the Ph.D. Dissertation written by
Ji Won Woo
January 2022

Chair	_____(Seal)
Vice Chair	_____(Seal)
Examiner	_____(Seal)
Examiner	_____(Seal)
Examiner	_____(Seal)

유방암 조직의
포괄적인 면역 프로파일링과
S100A8 양성 면역세포의 의의 분석

지도교수 박 소 연

이 논문을 의학박사 학위논문으로 제출함

2021년 10월

서울대학교 대학원

의학과 병리학전공

우 지 원

우지원의 의학박사 학위논문을 인준함

2022년 1월

위 원 장 _____(인)

부위원장 _____(인)

위 원 _____(인)

위 원 _____(인)

위 원 _____(인)

ABSTRACT

Background: Immune microenvironment differs according to hormone receptor (HR) status or tumor progression stage. Its importance is ever-increasing as drugs targeting tumor immunity came up as a game changer in cancer therapeutics. Myeloid-derived suppressor cells (MDSCs) are one of the key players in tumor immunity but not well studied in human tissue because of its phenotypic complexity. They are known to promote tumor progression via various immune-mediated and non-immune-mediated mechanisms.

Methods: Differential expression of immune-related genes was evaluated via comprehensive immune profiling according to unsupervised clustering and HR status, and a target gene with significant fold change, possibly MDSC-associated gene, was searched for further analysis. The difference in its expression was validated using tissue microarray of 700 cases of human breast cancer. Its clinicopathological significance and relationship between other tumor infiltrating lymphocytes (TILs) including CD4+, CD8+ and FOXP3+ TILs or PD-L1+ immune cells (ICs) were investigated.

Results: In immune profiling analysis, S100A8, a known MDSC marker, showed the most striking fold change in the cluster 2 in unsupervised clustering and HR status dependent grouping. In immunohistochemistry (IHC), S100A8 was stained in both tumor cells and ICs in breast cancer samples. Infiltration of S100A8+ ICs was associated with aggressive clinicopathological features and poor clinical outcome. They were already present in pre-invasive stage of breast cancer and were associated with increased infiltration of CD4+, CD8+, and FOXP3+ TILs and PD-L1+ ICs. Prognostic impact of S100A8+ ICs was stronger in HR-positive, PD-L1+ IC-negative, CD8+ TIL-low and FOXP3+ TIL-low subgroups. When stained with various IHC markers, S100A8+ ICs were mostly revealed as CD33+ CD15-CD163+ cells which are thought to be monocytic-MDSCs derived macrophages.

Conclusion: S100A8 is a key molecule that differentiates distinct immune clusters and also highly expressed in HR-negative breast cancers. S100A8 is usually expressed in monocytic-MDSCs derived macrophages and contributes to breast cancer progression from pre-invasive stage. S100A8+ ICs were associated with increase in CD4+, CD8+, and FOXP3+ TILs and PD-L1+ ICs but prognostic impact of S100A8+ ICs was stronger in less immunogenic condition.

Keyword: S100A8, invasive breast cancer, myeloid derived suppressor cell, tumor immune microenvironment, tumor associated macrophage

Student Number: 2018-22261

TABLE OF CONTENTS

LIST OF TABLES

LIST OF FIGURES

LIST OF SUPPLEMENTARY TABLES

LIST OF ABBREVIATIONS

MDSC	myeloid derived suppressor cell
PMN-MDSC	polymorphonuclear myeloid derived suppressor cell
M-MDSC	monocytic myeloid derived suppressor cell
TAM	tumor associated macrophages
TIL	tumor infiltrating lymphocyte
HR	hormone receptor
ER	estrogen receptor
PR	progesterone receptor
HER2	human epidermal growth factor receptor 2
TNBC	triple negative breast cancer
TC	tumor cell
IC	immune cell
LVI	lymphovascular invasion
DEG	differentially expressed gene
FFPE	formalin fixed, paraffin embedded
TMA	tissue microarray
IHC	immunohistochemistry
ROC	receiver operating characteristic

1. Introduction

Breast cancer is the most commonly diagnosed cancer in women in worldwide [1] as well as in Republic of Korea [2] with increasing incidence. It is categorized into three major subtypes based on the expression of basic biomarkers including estrogen receptor (ER), progesterone receptor (PR) and human epidermal growth factor 2 (HER2) [3]: hormone receptor (HR) positive/HER2 negative, HER2 positive, and triple negative breast cancer (TNBC). Depending on the status of basic biomarkers and stage of the disease, patients receive tailored combinations of surgical resection, endocrine therapy, HER2-targeted treatment, chemotherapy or radiotherapy. In addition to these conventional methods of treatment, immunotherapy recently appeared as a revolutionary game changer in cancer therapeutics.

Some previous studies [4-6] have tried to figure out the different immune microenvironment according to breast cancer subtypes. O'Meara et al. [4] compared a subset of ER-positive breast cancer that contains high levels of tumor infiltrating lymphocytes (TILs) with immune-rich TNBCs and observed more attenuated immune microenvironment in immune-rich ER-positive breast cancers mediated by increased TGF-β signaling and M2 macrophage presence. Sadeghalvad et al. [5] summarized in their review article that the distribution of immune cells and their presumptive roles are different among distinct molecular subtypes of breast cancer. Regulatory T cells, myeloid-derived suppressor cells (MDSCs), M2 macrophages were related to more immunosuppressive microenvironment and in contrast, NK cells and cytotoxic T lymphocytes were associated to the anti-tumor activity. These studies concluded that immune microenvironment of breast cancer is diverse and its diversity is associated with HR or HER2 status.

The immune microenvironment of in situ and invasive breast cancer is different as well. Trinh et al. [7] showed coevolution of cancer cells and the

immune microenvironment during cancer progression: Immune microenvironment became less active during in situ to invasive breast cancer transition but a spectrum of immune hot and cold tumors and a subtype specific difference were observed as early as in ductal carcinoma in situ.

So far, studies on tumor immunity have mainly focused on TILs, B and T lymphocytes and their interactions with the tumor. However, the tumor immunity cannot be explained solely by lymphoid cells and that there must be other players like neutrophils, NK cells, macrophages or MDSCs [8]. Among them, MDSCs were of major interest because of their diverse and powerful role in tumor promotion. MDSCs are known to suppress anti-tumor immunity by various mechanisms such as depleting nutrients required by lymphocytes, generating oxidative stress, interfering with lymphocyte trafficking and viability, activating and expanding regulatory T cell populations, decreasing effector T cell function, and inducing PD-L1 expression [9-11]. Furthermore, MDSCs are involved in tumor progression through non-immune-mediated mechanisms: they stimulate neovascularization by secreting vascular endothelial growth factor (VEGF) and basic fibroblast growth factor (bFGF) [12] and promote tumor invasion and metastasis via production of matrix metalloproteinases (MMP) and chemokines [13, 14].

While the importance of MDSCs in tumor progression cannot be overstated, its expression in human tissue remains vague due to its phenotypic complexity. MDSCs can be divided into two major subsets which have different functions: polymorphonuclear MDSCs (PMN-MDSCs) [CD11b+ (CD33+) CD14- CD15+] and monocytic MDSCs (M-MDSCs) [CD11b+ (CD33+) HLA-DRlow/- CD14+ CD15-] [15]. Most studies on MDSCs have focused on cells in peripheral lymphoid organs and peripheral blood, mainly due to technical challenges associated with MDSC isolation from tumors. Tumor MDSCs, however, are known to be different from peripheral MDSCs with a stronger immunosuppressive activity

[10].

In this study, differential expression of immune-related genes was evaluated via comprehensive immune profiling using NanoString nCounter method [16] according to unsupervised clustering and HR status. Target genes with significant fold change were searched for next step. As a result, S100A8, which is a well-known marker of MDSCs, revealed the highest level of difference in gene expression in the cluster 2 in unsupervised clustering and HR status dependent grouping. The difference in expression of S100A8 in tumor cells (TCs) and immune cells (ICs) was validated using immunohistochemistry between HR-positive and HR-negative breast cancers, and its clinicopathological significance was investigated in pre-invasive and invasive carcinoma of the breast. The relationship between S100A8+ ICs and other TIL subset infiltration including CD4+, CD8+, and FOXP3+ TILs and PD-L1+ ICs as well as the prognostic significance of S100A8+ ICs in various immune environments were analyzed. Finally, S100A8+ immune cell phenotype was investigated using various IHC markers.

2. Materials and methods

2.1. Immune profiling using NanoString nCounter assay

2.1.1. Study population

Primary breast cancers with sufficient amount of tumor tissue and fine fixation status were selected from 2009 to 2012 archives of the Department of Pathology, Seoul National University Bundang Hospital. A total of 48 breast cancer cases, 16 pre-invasive and 32 invasive carcinomas, were selected for the assay and representative tumor sections were used. Of the 16 pre-invasive carcinoma (ductal carcinoma in situ), 12 cases had microinvasive foci in other tumor sections. HR-positive and HR-negative tumors were intentionally selected in equal number. Medical records were reviewed for clinicopathologic information. Baseline characteristics of the selected cases are summarized in **Supplementary Table 1** and **Supplementary Table 2**. Definition of biomarker status is explained in detail in **2.2.2.**

2.1.2. RNA extraction

Formalin fixed, paraffin embedded (FFPE) tissue blocks were cut into 10μm thickness and areas with more than 70% of tumor cells were macrodissected for the RNA extraction. RecoverAll™ Total Nucleic Acid Isolation Kit (Ambion, Grand Island, NY, USA) was used according to the manufacturer's recommended protocol. To check quantity and quality of the extracted RNA, DS-11 Spectrophotometer (Denovix INC, Wilmington, DE, USA) and Fragment Analyzer (Advanced Analytical Technologies, Ankey, IA, USA) were used, respectively. One invasive carcinoma case with negative HR status was excluded from the analysis because of low RNA concentration and low binding affinity.

2.1.3. NanoString nCounter data collection

NanoString nCounter (NanoString Technologies, Seattle, WA, USA) multiplex

assay was performed using the isolated RNA. 100ng of RNA per sample were hybridized using PanCancer Immune Profiling Panel for human (NanoString Technologies), which includes 730 target genes and 40 housekeeping genes. Absolute read counts were digitally quantified by nCounter Digital Analyzer (NanoString Technologies) that reads the fluorescent barcodes. For each assay, a high-density scan encompassing 280 fields of view was performed. After taking the images of immobilized fluorescent reporters in the sample cartilage with a CCD camera, the data was collected using the nCounter Digital Analyzer.

2.2. Validation of S100A8 expression in tissue microarray

2.2.1. Tissue samples and microarray construction

A total of 700 cases of breast cancer, 176 pre-invasive and 524 invasive carcinomas, were included. All cases were primary breast cancer of female which were surgically resected at Seoul National University Bundang Hospital from 2003 to 2011. Following information of cases was retrieved from medical records: age, sex, type of therapy received before and after surgical resection, histologic diagnosis (by 2019 WHO classification), ER, PR and HER2 status, Ki-67 proliferation index and p53 overexpression. For invasive carcinoma cases, additional information about size of the tumor, histologic grade (by Nottingham combined histologic grading system), lymphovascular invasion, TNM stage (by 7th American Joint Committee on Cancer staging system), recurrence and patient survival was collected. Deaths unrelated to the breast cancer were separately annotated for the analysis. For pre-invasive carcinoma cases, data regarding extent of the tumor, nuclear grade, comedo-type necrosis and recurrence was added. Baseline characteristics of the included cases are summarized in **Supplementary Table 3** and **Supplementary Table 4**.

Histologic slides were reviewed to mark the most representative area of the tumor before constructing tissue microarray (TMA). For pre-invasive

carcinoma, one to three 4mm diameter tissue cores were arranged depending on the extent of the tumor. For invasive carcinoma, three 2mm diameter tissue cores were selected. TMA was constructed using a trephine apparatus (Superbiochips Laboratories, Seoul, Korea).

2.2.2. Evaluation of standard biomarkers and determination of breast cancer subtypes

Expression of the standard biomarkers including ER, PR, HER2, Ki-67 and p53 was evaluated from the surgical resection specimens at the time of pathologic diagnosis. Immunohistochemical (IHC) staining was carried out on representative sections of the FFPE tissue blocks using following antibodies: ER (clone SP1; 1:100; LabVision, Fremont, CA, USA), PR (clone PgR 636; 1:70; Dako, Carpinteria, CA, USA), HER2 (clone 4B5; ready to use; Ventana Medical Systems, Tucson, AZ, USA), Ki-67 (clone MIB-1; 1:250; Dako) and p53 (clone D07; 1:600; Dako).

ER and PR were considered positive when 10% or more than 10% of tumor nuclei were stained since it has been suggested that a majority of breast cancers with low (1-10%) ER expression are biologically similar to HR-negative tumors [17]. HR status was defined as positive when ER and/or PR is positive. HER2 status was defined as positive when HER2 IHC showed positive staining (3+) or HER2 in situ hybridization showed gene amplification. Ki-67 proliferation index was divided into low and high using a 20% cutoff for invasive carcinoma and a 10% cutoff for pre-invasive carcinoma. For p53, staining in 10% or more of the tumor nuclei was considered positive.

Simple breast cancer subtyping was done using standard biomarker profiles referring to 2011 St Gallen International Expert Consensus [18]. Each subtype is defined as follows: luminal A (ER+ and/or PR+, HER2-, Ki-67<14%), luminal B (ER+ and/or PR+, HER2-, Ki-67≥14%; ER+ and/or PR+, HER2+),

HER2+ (ER-, PR-, HER2+) and triple negative (ER-, PR-, HER2-).

2.2.3. Immunohistochemical staining and scoring of S100A8

IHC staining for S100A8 using anti-S100A8 antibody (clone EPR3554; 1:2000; Abcam, Cambridge, UK) was performed on TMAs. Staining condition was optimized in advance using positive, negative controls and serial dilution. Briefly, sections from the TMA blocks were submitted to routine IHC techniques including deparaffinization and rehydration in graded ethanol. Antigen retrieval was performed by immersing the slides in citrate buffer (pH 6.0) for 30 minutes in a steamer. Endogenous peroxidase activity was blocked with a 3% H_2O_2-methanol solution, and the slides were incubated in 10% normal goat serum for 30 minutes to prevent non-specific staining. Then the slides were incubated for 1 hour at room temperature with anti-S100A8 antibody. Thereafter, horseradish peroxidase-labeled polymer conjugated with secondary antibodies (DAKO Envision detection kit, Dako) were treated for 30 minutes. Diaminobenzidine was used as a chromogen and the sections were counterstained with Mayer's hematoxylin.

S100A8 expression was separately evaluated in tumor cells (TCs) and ICs by two pathologists blinded to clinicopathologic information. S100A8 expressing cells were determined as TCs or ICs by histologic findings such as the location (in the tumor cell nest vs. in the stroma), cellular morphology (epithelioid vs. monocytoid, stellate or spindle shaped), and nuclear features (atypical vs. bland-looking). In some case where the distinction is difficult, simultaneous comparison with conventional hematoxylin and eosin stained slides was performed.

For TCs, the percentage of positively stained TCs in all TCs was counted regardless of intensity or staining pattern (cytoplasmic, membranous, or nuclear) as a previous study reported that correlation with various clinicopathologic features was irrespective of the location of S100A9 staining [19]. Scoring was done as a continuous variable and later dichotomized to either S100A8+TC-negative or –

positive group. Dichotomization was done according to the cutoff value of 0% estimated by receiver operating characteristic (ROC) curve analysis that maximized the sum of sensitivity and specificity in predicting disease-specific survival.

S100A8+ ICs were evaluated referring to preexisting guidelines for PD-L1 expression evaluation in breast cancer [20]. Average percentage of expression was recorded as a proportion of the area occupied by the positively stained ICs of any intensity or morphology in the tumor area including intratumoral and stromal areas. In pre-invasive carcinomas, the stromal compartment was defined as the area of specialized stroma surrounding the involved ducts, or when unclear, as the area surrounding the ducts within 2 high-power fields [21, 22]. Areas with crush artifacts, necrosis, or hyalinization were excluded. Intravascular ICs were not evaluated. The values were recorded as a continuous variable and categorized afterwards to either S100A8+ IC-negative or –positive group with an optimal cutoff value of 5% from ROC curve analysis.

2.2.4. Immune cell subset data organization

The data of CD4+, CD8+, and FOXP3+ TILs and PD-L1+ ICs were adopted from previous studies [23, 24] for all of the cases of pre-invasive carcinoma and 307 cases of invasive carcinoma. Immunohistochemical staining had been carried out using the following antibodies: CD4 (clone SP35; ready to use; Dako), CD8 (clone C8/144B; ready to use; Dako), FOXP3 (clone 236A/E7; 1:100; Abcam) and PD-L1 (clone E1L3N; 1:100; Cell Signaling, Danvers, MA, USA). CD4+, CD8+, and FOXP3+ T cells had been counted in intratumoral and stromal areas as absolute numbers per high power field. Detailed information on the counting method of TILs is described in the previous studies [23, 24]. For further analyses, CD4+, CD8+, and FOXP3+ TIL counts were dichotomized into high and low infiltration groups using cutoff values obtained by ROC curve analyses. PD-L1+ ICs were

considered to be present when at least 1% of the tumor stromal area was occupied by PD-L1+ ICs.

2.3. Evaluation of phenotype of S100A8+ ICs

Though S100A8 is known as a MDSC marker [15], confirmation that S100A8 stained ICs in this study are authentic MDSCs is needed. Several IHC antibodies were stained in serial sections of FFPE tissue blocks from representative invasive breast cancer cases. While phenotypic markers of MDSC are complex and still controversial, S100A8, CD33 (PWS44; ready to use; Leica, Lincolnshire, IL, USA), CD15 (Carb-3; 1:100; Dako), and CD163 (MRQ-26; ready to use; Ventana) were used referring to previous articles [15, 25, 26]. All the antibodies were automatically stained using in-house protocol by BenchMark ULTRA system (Roche, Rotkreuz, Switzerland) autostainer. Incubation time of primary antibody was adjusted from 32 minutes to 1 hour for CD33 as staining was weak by standard methods.

2.4. Statistical analyses

In immune profiling using NanoString nCounter assay, analysis of raw mRNA data was performed using NanoString technologies nSolver analysis software version 4.0 and nCounter Advanced Analysis version 2.0 (NanoString Technologies). The mRNA expression data was normalized using housekeeping genes. R software was used for comparison of mRNA expression between groups. Difference in gene expression was presented as a log2 fold change, and *p* values were adjusted by Benjamini-Hochberg procedure.

Other statistical analyses were performed using SPSS version 25.0 for Windows (IBM Corp., ARMONK, NY, USA). The data of S100A8 expression in TCs and ICs, and CD4+, CD8+ and FOXP3+ TIL counts did not meet the assumption of normality and non-parametric tests were used. The difference in

continuous variables was analyzed by Mann-Whitney *U* test between two groups. For comparison of categorical variables, Chi-square or Fisher's exact test was used. Spearman's rank correlation test was used to assess the correlation between two variables. Survival curves were estimated by Kaplan-Meier method, and the significance was calculated by log-rank test. Cox proportional hazard model was used for multivariate analysis using a backward stepwise selection method. Hazard ratios and their 95% confidence intervals were calculated for the significant variables. All *p* values were two-sided, and *p* values less than 0.05 were considered statistically significant.

3. Results

3.1. Comprehensive immune profiling using NanoString nCounter assay

3.1.1. Unsupervised clustering

Figure 1 illustrates the heatmap of all the genes and samples that passed the quality check after normalization. It was scaled to give all genes equal variance and generated by unsupervised clustering. In both pre-invasive and invasive carcinoma, specific DEG patterns were observed and samples were largely grouped into three clusters. The clustering results did not clearly match with HR nor HER2 status. In cluster 1 on the rightmost column, the included genes were globally under-expressed compared to the other clusters. In cluster 3 on the leftmost column, on the other hand, many immune-related genes were highly expressed. Cluster 2 showed intermediate feature between cluster 1 and 3.

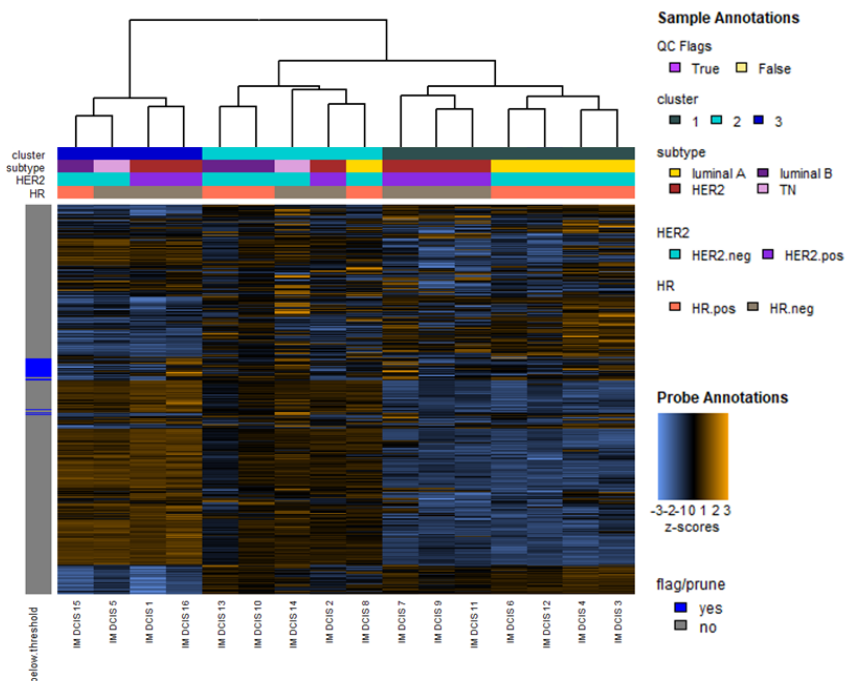

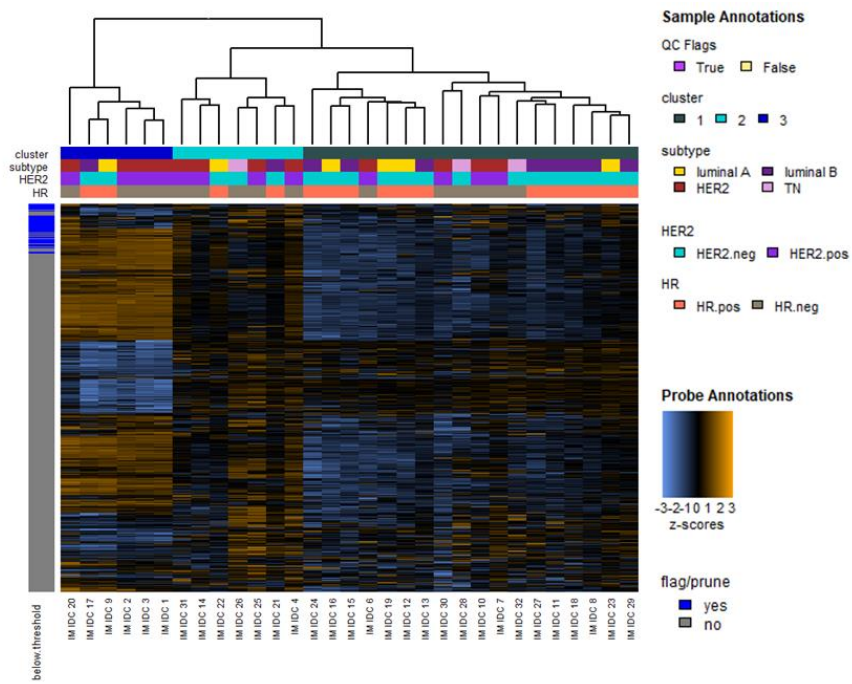

Figure 1. Heatmap of immune-related genes generated by unsupervised clustering in pre-invasive and invasive carcinoma. Normalized data was used, scaled to give all genes equal variance. The heatmap in the front is drawn from 16 samples of pre-invasive carcinoma and the heatmap at the back is drawn from 31 samples of invasive carcinoma. Color keys for sample annotation are arranged on the right. In either pre-invasive or invasive carcinoma, samples were grouped into distinct three clusters that were independent from breast cancer subtype, HER2 or hormone receptor status. Cluster 1 on the right is characterized by global low-expression of immune-related genes. Many immune-related genes were highly expressed in cluster 3 on the left. Cluster 2 showed borderline feature between cluster 1 and 3.

As a previous study [6] using the same immune profiling method showed that cluster with intermediate immune infiltration (cluster 2 in the present study) was associated with a worst prognosis, DEGs in cluster 2 were analyzed. **Table 1** and **Table 2** summarize top 20 genes with significant fold change and *p* value in cluster 2 of pre-invasive and invasive carcinoma compared to other clusters. In pre-invasive carcinoma, CCR9 showed the largest log2 fold change, 3.18, with adjusted *p* value of 0.456. Other genes had adjusted *p* values more than 0.5. In invasive carcinoma, S100A8 showed the largest log2 fold change, 3.66, with adjusted *p* value of 0.096. LTF, CD24, CCL5, CD79A, CD7 were also highly expressed in cluster 2 of invasive carcinoma with log2 fold change more than 2. **Figure 2** illustrates the distribution of DEGs in cluster 2 compared to other clusters in invasive carcinoma. Some of the genes in cluster 2 were commonly up-regulated in HR-negative cases as well. S100A8, LTF, CD24, CCL5, CD79A, IL34, MS4A1, LBP, CX3CL1, and DDX43 were also highly expressed in HR-negative cases.

Table 1. List of top 20 DEGs in the cluster 2 compared to other clusters in pre-invasive carcinoma

Gene (mRNA)	Log2 fold change	*p* value	Adjusted *p* value*
CCR9	3.18	0.001	0.456
HLA-B	2.75	0.008	0.547
HLA-DRB3	2.47	0.009	0.547
HLA-C	2.13	0.026	0.786
SYCP1	2.01	0.020	0.786
KIT	1.87	0.050	0.984
DUSP6	-1.6	0.025	0.786
DUSP4	-1.53	0.020	0.786
PSMB9	1.4	0.007	0.547
CEBPB	-1.3	0.025	0.786
TAP2	1.26	0.010	0.547
CCL5	1.14	0.009	0.547
JAK2	1.04	0.021	0.786
IFIH1	1.03	0.007	0.547
RORA	0.99	0.003	0.547
MICA	0.911	0.042	0.948
CD34	0.91	0.010	0.547
RIPK2	-0.883	0.042	0.948
TNFAIP3	0.847	0.020	0.786
FADD	0.798	0.026	0.786

* Adjusted by Benjamini-Hochberg procedure

Table 2. List of top 20 DEGs with significance in the cluster 2 compared to other clusters in invasive carcinoma

Gene (mRNA)	Log2 fold change	*p* value	Adjusted *p* value*
S100A8	3.66	0.003	0.096
LTF	3.59	<0.001	0.001
CD24	3.11	<0.001	0.008
CCL5	2.14	<0.001	0.071
CD79A	2.12	0.011	0.186
CD7	2.04	0.003	0.096
IL34	1.89	0.002	0.081
TNFRSF11A	1.86	0.006	0.142
MS4A1	1.84	0.009	0.184
MRC1	1.78	0.030	0.298
LBP	1.69	0.041	0.325
CX3CL1	1.68	0.016	0.220
CXCL9	1.68	0.017	0.222
SH2D1A	1.67	0.030	0.298
LAG3	1.66	0.037	0.317
JAK3	1.55	0.029	0.298
IL5	1.51	0.009	0.178
DDX43	1.49	0.025	0.270
CD59	1.47	0.003	0.089
TNFSF10	1.46	0.012	0.186

* Adjusted by Benjamini-Hochberg procedure

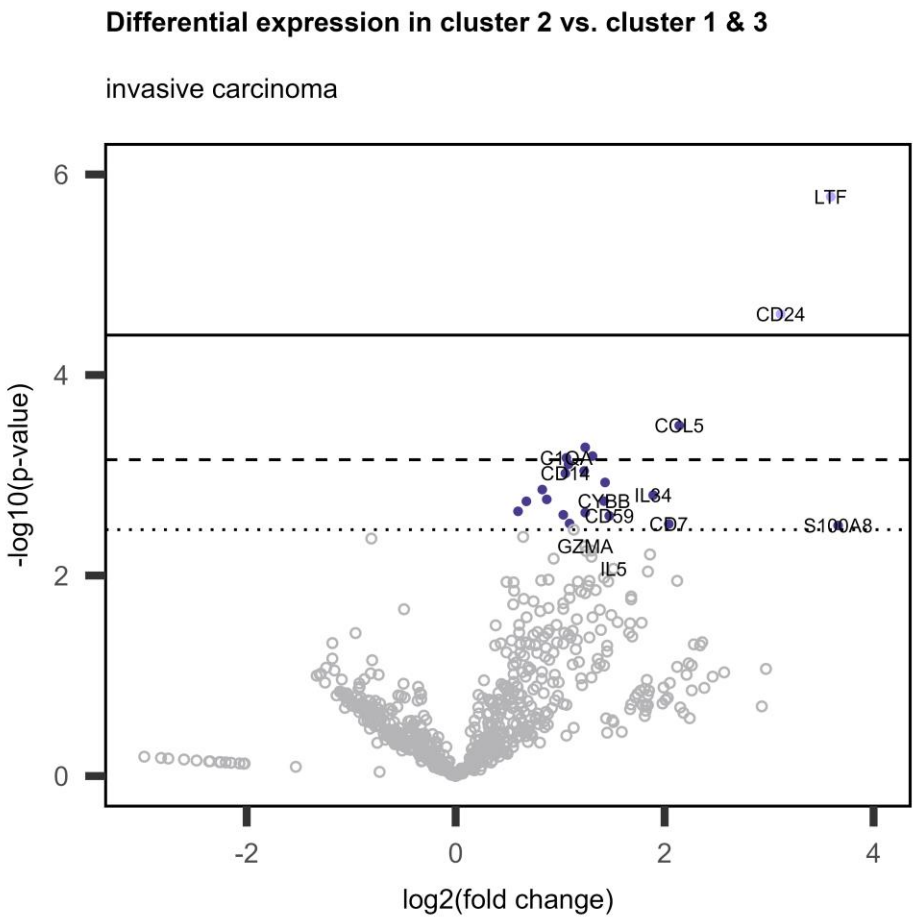

Figure 2. Volcano plot illustrating DEGs in the cluster 2 compared to the other clusters in invasive carcinoma. Genes with fold change more than 2 and unadjusted *p* value less than 0.01 are labeled. Dotted, dashed and solid horizontal line indicate adjusted *p* value 0.1, 0.05 and 0.01, respectively. S100A8 showed the largest fold change value among all the genes.

3.1.2. Comparison of immune-related gene expression in HR-positive and HR-negative tumors

Immune-related DEGs were analyzed according to HR status. **Table 3** and **Table 4** summarize top 20 genes with significant fold change and *p* value in pre-invasive and invasive carcinoma groups, respectively. In pre-invasive carcinoma, S100A8, S100A7, CSF3, LBP, LCN2, LTB, CXCL1, TNFRSF12A were up-regulated and IGF1R, CFD, IL6ST, IFITM1, FOS, CD36, BCL2, SERPING1, IKBKB, TNFRSF14, BMI1, CSF1 were down-regulated in HR-negative tumors compared to the HR-positive ones. In invasive carcinoma, LCN2, S100A8, LTF, IL34, MARCO, CD24, DDX43, CX3CL1, CXCL10, CD79A, CCL18, CD19, IDO1, SLAMF6, CXCL1, MS4A1, CCL5 were up-regulated and IGF1R, GATA3, IL6ST were down-regulated in HR-negative tumors compared to the HR-positive ones.

Figure 3 demonstrates distribution of differential expression data of immune-related genes in volcano plot. Log2 fold changes were calculated using HR-positive cases as the baseline. S100A8, IGF1R, LCN2, IL6ST and CXCL1 expression showed significant fold change in both pre-invasive and invasive carcinoma groups. They all showed absolute log2 fold change more than 1.5 and adjusted *p* value less than 0.05. While S100A8, LCN2 and CXCL1 expression was increased in HR-negative group, IGF1R and IL6ST expression was decreased. Among the genes, S100A8 was the most striking DEG with fold change value of 5.81 (adjusted $p = 0.001$) and 3.18 (adjusted $p = 0.041$) in pre-invasive and invasive carcinoma groups, respectively.

Table 3. List of top 20 DEGs with significance according to HR status in pre-invasive carcinoma

Gene (mRNA)	Log2 fold change*	*p* value	Adjusted *p* value**
S100A8	5.81	<0.001	0.001
S100A7	4.03	<0.001	0.030
CSF3	3.24	0.003	0.079
IGF1R	-2.87	<0.001	0.001
CFD	-2.46	0.001	0.041
IL6ST	-2.45	<0.001	0.006
IFITM1	-2.43	0.001	0.049
LBP	2.43	0.002	0.076
FOS	-2.41	0.001	0.049
LCN2	2.36	0.001	0.041
LTB	2.19	0.001	0.049
CD36	-2.16	0.001	0.049
BCL2	-2.03	<0.001	0.011
CXCL1	1.97	<0.001	0.034
TNFRSF12A	1.71	0.002	0.063
SERPING1	-1.63	0.003	0.079
IKBKB	-1.61	0.001	0.041
TNFRSF14	-1.6	<0.001	0.034
BMI1	-1.5	0.002	0.066
CSF1	-1.44	0.003	0.076

*Log2 fold changes were calculated using HR-positive tumors as the baseline; **Adjusted by Benjamini-Hochberg procedure

Table 4. List of top 20 DEGs with significance according to HR status in invasive carcinoma

Gene (mRNA)	Log2 fold change*	*p* value	Adjusted *p* value**
LCN2	3.42	<0.001	0.011
S100A8	3.18	0.002	0.041
LTF	2.57	<0.001	0.014
IGF1R	-2.53	<0.001	<0.001
IL34	2.53	<0.001	0.011
MARCO	2.32	<0.001	0.013
CD24	2.27	0.001	0.028
DDX43	2.26	0.002	0.036
CX3CL1	2.24	<0.001	0.008
CXCL10	2.09	0.002	0.041
GATA3	-2.08	<0.001	<0.001
CD79A	1.99	0.005	0.058
CCL18	1.98	<0.001	0.022
CD19	1.97	<0.001	0.008
IDO1	1.96	0.001	0.024
SLAMF6	1.79	<0.001	0.013
IL6ST	-1.75	<0.001	<0.001
CXCL1	1.72	0.001	0.030
MS4A1	1.69	0.005	0.057
CCL5	1.67	0.001	0.035

*Log2 fold changes were calculated using HR-positive cases as the baseline; **Adjusted by Benjamini-Hochberg procedure

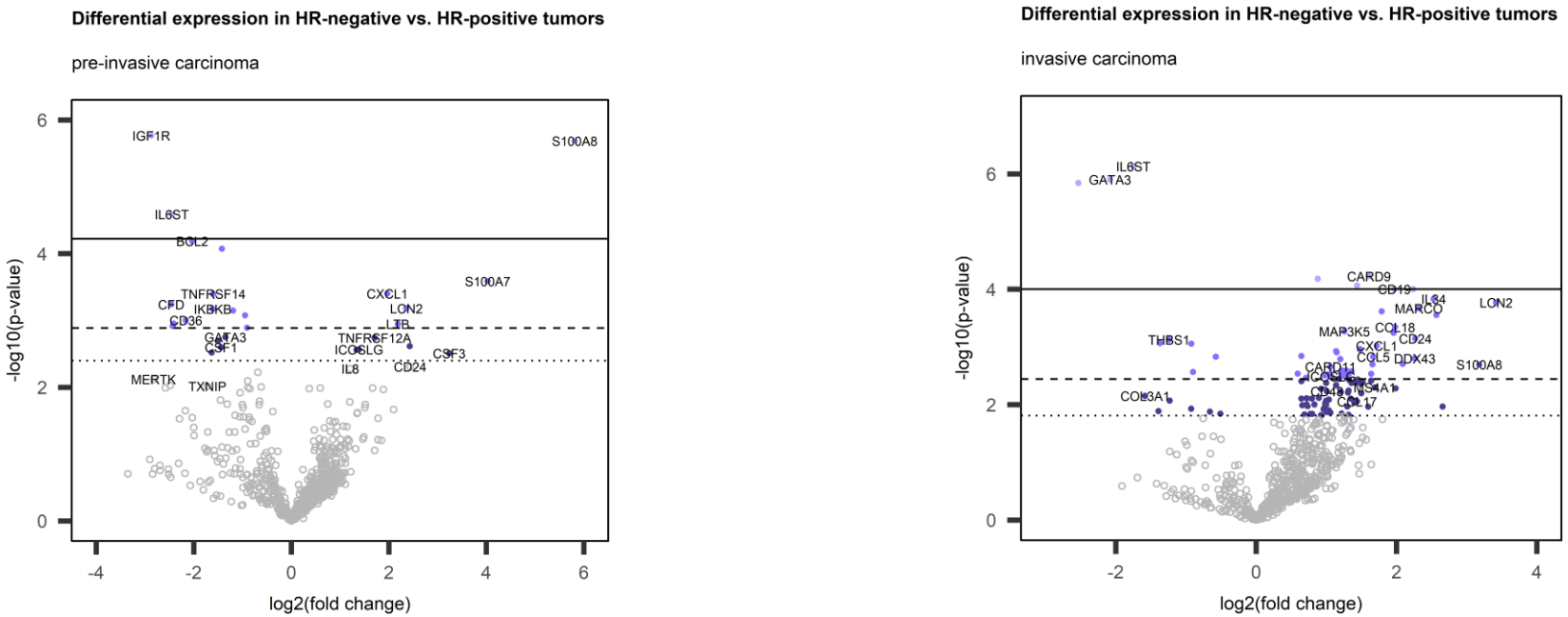

Figure 3. Volcano plots showing DEGs according to HR status in pre-invasive and invasive carcinoma. Log2 fold changes were calculated using HR-positive cases as the baseline. Genes with fold change more than 2 and unadjusted *p* value less than 0.01 are labeled. Dotted, dashed and solid horizontal line indicate adjusted *p* value 0.1, 0.05 and 0.01, respectively. In pre-invasive carcinoma group, S100A8 showed fold change 5.81 with adjusted *p* value 0.001. In invasive carcinoma group, S100A8 showed fold change 3.18 with adjusted *p* value 0.041.

3.2. Evaluation of S100A8 expression in breast cancer using tissue microarray

3.2.1. Validation of S100A8 differential expression according to hormone receptor status

S100A8 was well stained in both TCs and ICs of pre-invasive and invasive carcinomas. Representative images of S100A8 IHC staining are demonstrated in **Figure 4**. In pre-invasive carcinoma, S100A8 expression was detected in up to 90% of TCs, and S100A8+ ICs were found in up to 50% of a tumor area. In invasive carcinoma, S100A8+ TCs comprised up to 100% of TCs, and S100A8+ ICs were also found in up to 50% of a tumor area. S100A8 expression in TCs and ICs showed a weak positive correlation in pre-invasive carcinoma (rho=0.260) and a moderate positive correlation in invasive carcinoma (rho=0.452) as shown in the scatter plots (**Figure 5**).

First, the differential expression of S100A8 was validated by IHC using tissue microarrays according to HR status (**Table 5**). In HR-positive tumors, S100A8 was usually stained in ICs and rarely stained in TCs. In HR-negative tumors, on the other hand, both TCs and ICs showed substantial expression. The proportions of S100A8+ TCs and ICs were significantly higher in HR-negative tumors compared to HR-positive ones in total and invasive carcinoma groups (all $p<0.001$). In pre-invasive carcinoma, the proportion of S100A8+ TCs was also higher ($p<0.001$) in HR-negative subgroup than in HR-positive subgroup, while S100A8+ ICs showed borderline difference between the two group ($p=0.100$).

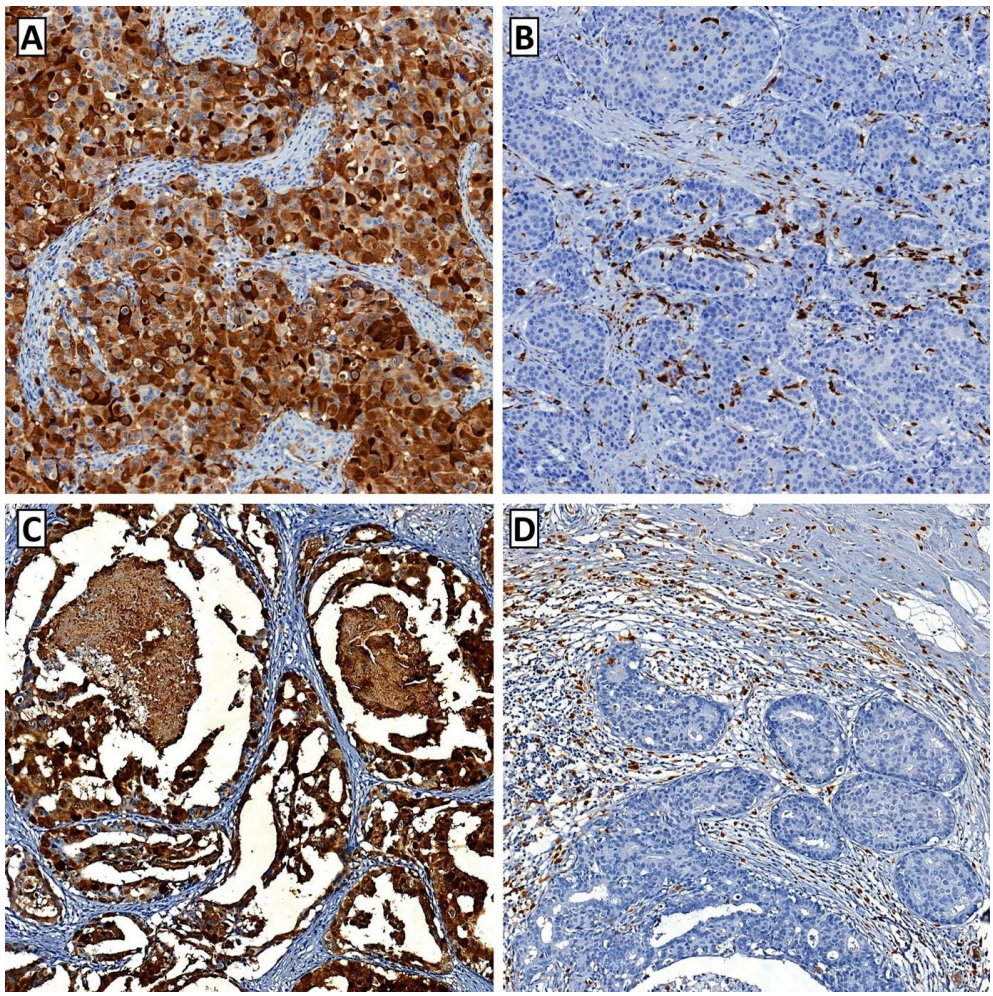

Figure 4. Representative images of S100A8 IHC staining in breast cancer. **A** Tumor cells showed strong cytoplasmic expression of S100A8 in a HR-negative invasive breast carcinoma. S100A8+ ICs of stromal area were rarely found in this case. **B** A case of HR-positive invasive breast carcinoma showed frequent S100A8+ ICs, whereas tumor cells were totally negative for S100A8. **C** In a case of high-grade ductal carcinoma in situ with comedo-type necrosis, the tumor cells showed strong S100A8 expression. HR status was negative in this case. **D** In this case of HR-positive ductal carcinoma in situ, abundant S100A8+ ICs were found in association with numerous tumor-infiltrating lymphocytes. Tumor cells were negative for S100A8 expression.

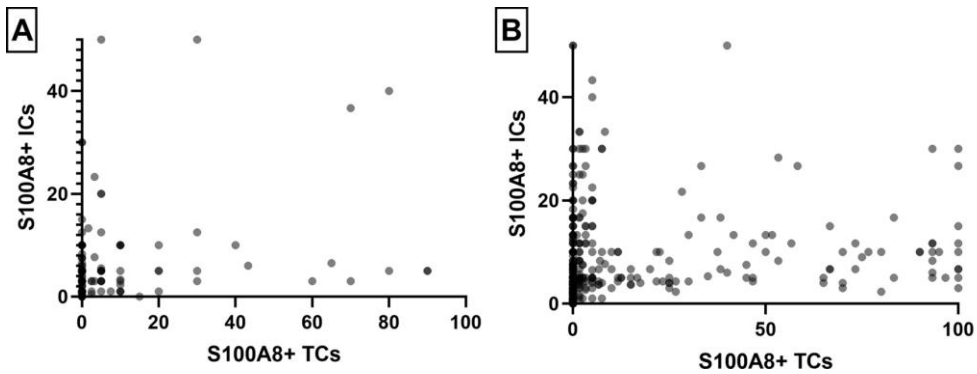

Figure 5. Scatter plots showing the relationship between S100A8+ TCs and S100A8+ ICs. **A** In pre-invasive carcinoma, S100A8+ TCs and S100A8+ ICs showed a weak positive correlation (rho=0.260). **B** In invasive carcinoma, S100A8+ TCs and S100A8+ ICs were moderately correlated (rho=0.452).

Table 5. Comparison of S100A8 expression between HR positive and negative groups

	HR+ subgroup	HR- subgroup	*p* value
Total			
S100A8+ TC (%)	0.00 (0.00-0.00)	5.00 (0.00-39.17)	<0.001
S100A8+ IC (%)	3.00 (1.33-5.00)	7.00 (4.33-13.33)	<0.001
Pre-invasive carcinoma			
S100A8+ TC (%)	0.00 (0.00-0.00)	10.00 (8.75-36.67)	<0.001
S100A8+ IC (%)	3.00 (1.00-5.00)	5.00 (2.000-9.17)	0.100
Invasive carcinoma			
S100A8+ TC (%)	0.00 (0.00-0.00)	5.00 (0.00-40.00)	<0.001
S100A8+ IC (%)	3.33 (1.67-5.00)	7.67 (4.33-15.00)	<0.001

P values are calculated by Mann-Whitney *U* test.

Data are presented as median value (interquartile range).

3.2.2. S100A8+ tumor cells and immune cells in pre-invasive and invasive carcinoma

Next, the difference in S100A8 expression between pre-invasive and invasive carcinoma was additionally analyzed (**Table 6**). S100A8+ ICs were significantly higher in invasive carcinomas than in pre-invasive carcinomas (p=0.010), whereas S100A8+ TCs did not show significant difference between the two (p=0.544). In subgroup analysis by HR status, the difference in S100A8+ ICs was also apparent in HR-negative subgroup (p=0.014) but not in HR-positive subgroup (p=0.872). The proportion of S100A8+ TCs did not differ between pre-invasive and invasive carcinomas in the HR-positive subgroup (p=0.228); however, it tended to be higher in pre-invasive carcinomas than in invasive carcinomas in the HR-negative subgroup (p=0.081).

Table 6. Comparison of S100A8 expression between pre-invasive carcinoma and invasive carcinoma

	Pre-invasive carcinoma	Invasive carcinoma	*p* value
Total			
S100A8+ TC (%)	0.00 (0.00-5.00)	0.00 (0.00-2.63)	0.544
S100A8+ IC (%)	3.00 (1.00-5.00)	4.33 (2.33-8.33)	0.010
HR+ subgroup			
S100A8+ TC (%)	0.00 (0.00-0.00)	0.00 (0.00-0.00)	0.228
S100A8+ IC (%)	3.00 (1.00-5.00)	3.33 (1.67-5.00)	0.872
HR- subgroup			
S100A8+ TC (%)	10.00 (8.75-36.67)	5.00 (0.00-40.00)	0.081
S100A8+ IC (%)	5.00 (2.00-9.17)	7.67 (4.33-15.00)	0.014

P values are calculated by Mann-Whitney *U* test.

Data are presented as median value (interquartile range).

3.2.3. S100A8+ tumor cells and immune cells in relation to clinicopathologic features

Relationships between the presence of S100A8+ TCs or ICs and various clinicopathologic features of the tumors are summarized in **Tables 7** and **8**. In pre-invasive carcinoma, the presence of S100A8+ TCs was associated with aggressive clinicopathologic features of tumor including a large extent of tumor, high nuclear grade, comedo-type necrosis, ER negativity, PR negativity, positive HER2 status, high Ki-67 index, and p53 overexpression (all $p<0.05$). Infiltration of S100A8+ ICs showed an association with only ER negativity ($p=0.030$) and tended to be associated with comedo-type necrosis ($p=0.081$) and high Ki-67 index ($p=0.087$). In invasive carcinoma, the presence of S100A8+ TCs and ICs was commonly associated with high histologic grade, ER negativity, PR negativity, HER2 positivity, and p53 overexpression (all $p<0.001$). Borderline association with pathologic T ($p=0.064$) and N stage ($p=0.068$) was present in S100A8+ ICs but not in S100A8+ TCs.

Table 7. Relationship between S100A8 expression in TCs and ICs and clinicopathological features of pre-invasive carcinoma

Clinicopathological feature	S100A8+ TC		*p* value	S100A8+ IC		*p* value
	Negative	Positive		Negative	Positive	
Extent			0.012			0.238
<3.2cm	61 (50.0)	38 (70.4)		49 (52.1)	50 (61.0)	
≥3.2cm	61 (50.0)	16 (29.6)		45 (47.9)	32 (39.0)	
Nuclear grade			0.004			0.594
Low	10 (8.2)	1 (1.9)		7 (7.4)	4 (4.9)	
Intermediate	75 (61.5)	23 (42.6)		54 (57.4)	44 (53.7)	
High	37 (30.3)	30 (55.6)		33 (35.1)	34 (41.5)	
Comedo-type necrosis			0.027			0.081
Absent	98 (80.3)	35 (64.8)		76 (80.9)	57 (69.5)	
Present	24 (19.7)	19 (35.2)		18 (19.1)	25 (30.5)	
ER			<0.001			0.030
Positive	119 (97.5)	35 (64.8)		87 (92.6)	67 (81.7)	
Negative	3 (2.5)	19 (35.2)		7 (7.4)	15 (18.7)	
PR			<0.001			0.389
Positive	110 (90.2)	24 (44.4)		74 (78.7)	60 (73.2)	
Negative	12 (9.8)	30 (55.6)		20 (21.3)	22 (26.8)	
HER2 status			0.001			0.147
Negative	112 (91.8)	39 (72.2)		84 (89.4)	67 (81.7)	
Positive	10 (8.2)	15 (27.8)		10 (10.6)	15 (18.3)	
Ki67 index			0.036			0.087
Low (<10%)	111 (91.0)	43 (79.6)		86 (91.5)	68 (82.9)	
High (≥10%)	11 (9.0)	11 (20.4)		8 (8.5)	14 (17.1)	
P53 overexpression			0.005			0.134
Absent	113 (92.6)	42 (77.8)		86 (91.5)	69 (84.1)	
Present	9 (7.4)	12 (22.2)		8 (8.5)	13 (15.9)	
Subtype			<0.001			0.215
Luminal A	101 (82.8)	26 (48.1)		73 (77.7)	54 (65.9)	
Luminal B	18 (14.8)	10 (18.5)		14 (14.9)	14 (17.1)	
HER2+	1 (0.8)	7 (13.0)		3 (3.2)	5 (6.1)	
Triple negative	2 (1.6)	11 (20.4)		4 (4.3)	9 (11.0)	

P values are calculated by Chi-square or Fisher's exact test. Number in parenthesis indicates percentage.

Table 8. Relationship between S100A8 expression in TCs and ICs and clinicopathological features of invasive carcinoma

Clinicopathological features	S100A8+ TC		*p* value	S100A8+ IC		*p* value
	Negative	Positive		Negative	Positive	
T stage			0.689			0.064
T1	166 (47.6)	80 (45.7)		142 (50.7)	104 (42.6)	
T2-T4	183 (52.4)	95 (54.3)		138 (49.3)	140 (57.4)	
N stage			0.880			0.068
N0	199 (57.0)	101 (57.7)		150 (53.6)	150 (61.5)	
N1-N3	150 (43.0)	74 (42.3)		130 (46.4)	94 (38.5)	
Histologic grade			<0.001			<0.001
Low	85 (24.4)	9 (5.1)		72 (25.7)	22 (9.0)	
Intermediate	136 (39.0)	30 (17.1)		124 (44.3)	42 (17.2)	
High	128 (36.7)	136 (77.7)		84 (30.0)	180 (73.8)	
LVI			0.557			0.393
Absent	194 (55.6)	102 (58.3)		163 (58.2)	133 (54.5)	
Present	155 (44.4)	73 (41.7)		117 (41.8)	111 (45.5)	
ER			<0.001			<0.001
Positive	287 (82.2)	66 (37.7)		236 (84.3)	117 (48.0)	
Negative	62 (17.8)	109 (62.3)		44 (15.7)	127 (52.0)	
PR			<0.001			<0.001
Positive	227 (65.0)	51 (29.1)		187 (66.8)	91 (37.3)	
Negative	122 (35.0)	124 (70.9)		93 (33.2)	153 (62.7)	
HER2 status			<0.001			<0.001
Negative	56 (16.0)	64 (36.6)		42 (15.0)	78 (32.0)	
Positive	293 (84.0)	111 (63.4)		238 (85.0)	166 (68.0)	
Ki67 index			<0.001			<0.001
Low	248 (71.1)	53 (30.3)		214 (76.4)	87 (35.7)	
High	101 (28.9)	122 (69.7)		66 (23.6)	157 (64.3)	
P53 overexpression			<0.001			<0.001
Absent	286 (81.9)	100 (57.1)		232 (82.9)	154 (63.1)	
Present	63 (18.1)	75 (42.9)		48 (17.1)	90 (36.9)	
Subtype			<0.001			<0.001
Luminal A	195 (55.9)	30 (17.1)		169(60.4)	56 (23.0)	
Luminal B	96 (27.5)	43 (24.6)		71 (25.4)	68 (27.9)	
HER2+	19 (5.4)	45 (25.7)		16 (5.7)	48 (19.7)	
Triple negative	39 (11.2)	57 (33.4)		24 (8.6)	72 (29.5)	

P values are calculated by Chi-square or Fisher's exact test. Number in parenthesis indicates percentage.

3.2.4. Impact of S100A8+ tumor cells and immune cells on clinical outcome of the patients

Next, the patients' clinical outcome was evaluated in relation to the presence of S100A8+ TCs or infiltration of S100A8+ ICs in pre-invasive and invasive carcinomas. As for patients with pre-invasive carcinoma, the mean follow-up period was 6.7 years (standard deviation, 3.0 years) during which 8 patients developed ipsilateral breast recurrence. In survival analyses, infiltration of S100A8+ ICs, but not the presence of S100A+ TCs, was associated with ipsilateral breast recurrence (p=0.011, p=0.495, respectively; **Figure 6**). In subgroup analyses according to HR status, infiltration of S100A8+ ICs was associated with ipsilateral breast recurrence in the HR-positive subgroup, but not in the HR-negative subgroup (p=0.028, p=0.350, respectively; **Figure 6**).

In patients with invasive carcinoma, the mean follow-up period was 9.4 years (standard deviation, 4.0 years) during which 32 patients revealed cancer-related death. In survival analyses, the presence of S100A8+ TCs and infiltration of S100A8+ ICs were associated with poor disease-specific survival (p=0.005, p=0.003, respectively; **Figure 7**). The same difference in survival was also observed in HR-positive subgroup (S100A8+ TCs, p=0.015; S100A8+ ICs, p=0.029; **Figure 7**). However, in HR-negative subgroup, there was no statistical difference in disease-specific survival in relation to S100A8+ TCs or ICs (p=0.956, p=0.485, respectively; **Figure 7**). In multivariate analyses (**Table 9**), infiltration of S100A8+ ICs (p=0.041) was revealed as an independent poor prognostic factor along with nodal metastasis, lymphovascular invasion, and HR negativity (p=0.019, p=0.048, p=0.013, respectively). However, S100A8+ TC was not proven an independent prognostic factor (p=0.237).

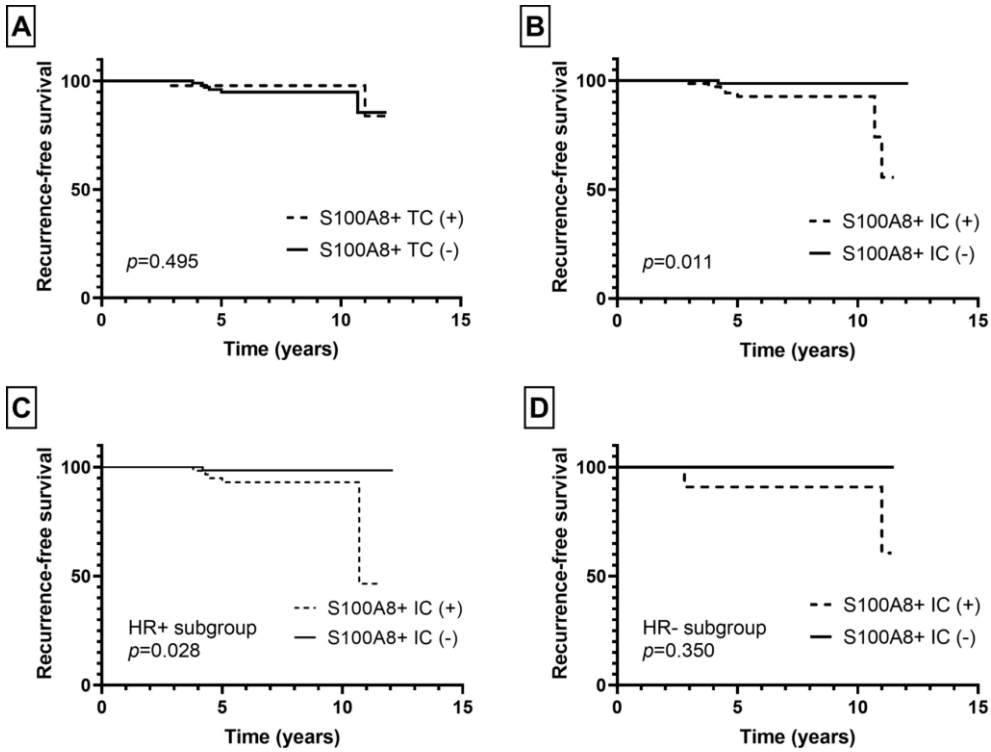

Figure 6. Kaplan-Meier survival curves according to S100A8+ TC and S100A8+ IC in pre-invasive carcinoma. **A** S100A8+ TC was not associated with ipsilateral breast recurrence. **B** Infiltration of S100A8+ IC showed association with decreased recurrence-free survival (p=0.011). **C** In subgroup analysis, HR-positive subgroup analysis revealed association between S100A8+ IC and poor recurrence-free survival (p=0.028). **D** In HR-negative subgroup, S100A8+ IC was not associated with recurrence-free survival.

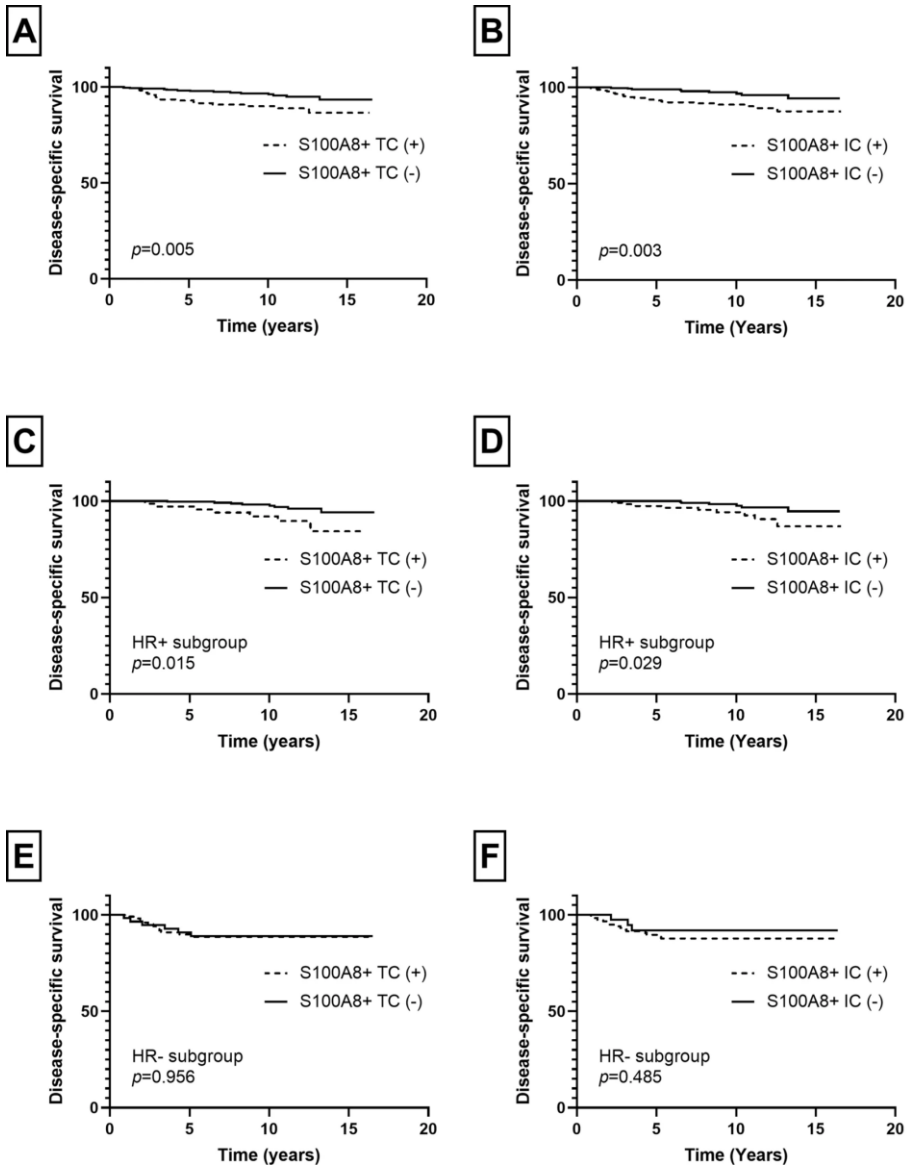

Figure 7. Kaplan-Meier survival curves according to S100A8+ TC and S100A8+ IC in invasive carcinoma. **A, B** As a whole, presence of S100A8+ TC (p=0.005) and infiltration of S100A8+ IC (p=0.003) were associated with poor disease-specific survival. **C, D** In HR-positive subgroup, both S100A8+ TC (p=0.015) and S100A8+ IC (p=0.029) showed association with poor disease-specific survival as well. **E, F** In HR-negative subgroup, however, there was no statistical difference in survival despite difference in expression of S100A8+ TC or S100A8+ IC.

Table 9. Univariate and multivariate analyses of disease-specific survival in invasive carcinoma

Variable	Category	Univariate analysis		Multivariate analysis	
		HR (95% CI)	***p-value***	**HR (95% CI)**	***p-value***
Age	<50 years vs. ≥50 years	0.818 (0.407-1.664)	0.572	-	-
T stage	T1 vs. T2-4	2.193 (1.014-4.743)	0.046	1.377 (0.615-3.083)	0.437
N stage	N0 vs. N1-N3	3.187 (1.474-6.895)	0.003	2.761 (1.184-6.437)	0.019
Histologic grade	I & II vs. III	2.644 (1.223-5.716)	0.013	1.527 (0.612-3.811)	0.364
LVI	Absent vs. Present	3.280 (1.517-7.091)	0.003	2.342 (1.008-5.444)	0.048
Hormone receptor	Negative vs. Positive	0.369 (0.184-0.738)	0.005	0.390 (0.186-0.820)	0.013
HER2	Negative vs. Positive	1.158 (0.520-2.579)	0.719	-	-
Ki-67 index	Low vs. High	2.058 (1.016-4.167)	0.045	0.822 (0.324-2.086)	0.680
S100A8+ TCs	Negative vs. Positive	2.594 (1.290-5.215)	0.007	1.594 (0.736-3.452)	0.237
S100A8+ ICs	Negative vs. Positive	3.017 (1.396-6.522)	0.005	2.345 (1.034-5.316)	0.041

HR, hazard ratio; CI, confidence interval

As S100A8 expression in TCs and ICs was not always concordant, survival analyses were performed using the combination of S100A8+ TCs and ICs. Disease-specific survival was different among the four combined groups (p=0.009; **Figure 8**) with the best clinical outcome belonging to S100A8+ TC (-)/S100A8+ IC (-) group. However, there was no difference in survival among S100A8+ TC (+)/S100A8+ IC (-) group, S100A8+ TC (-)/S100A8+ IC (+) group, or S100A8+ TC (+)/S100A8+ IC (+) group.

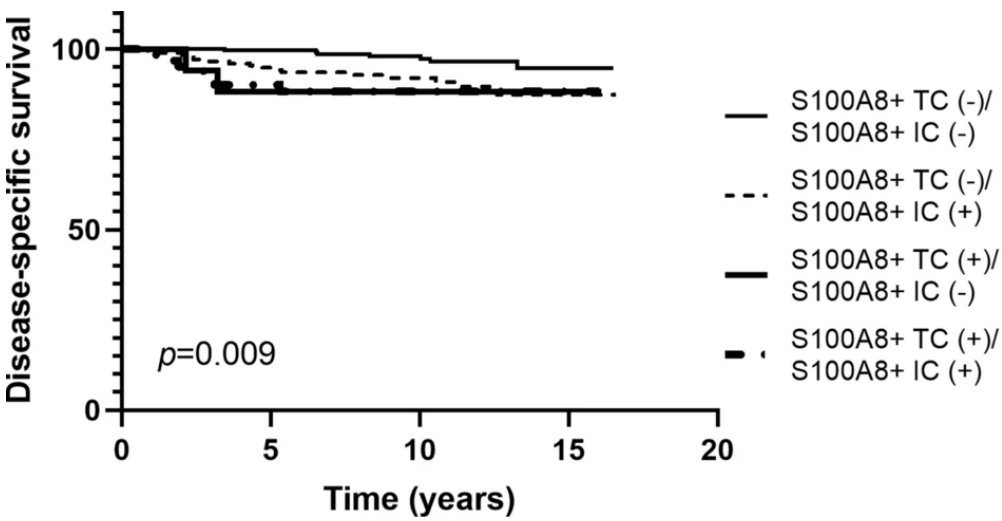

Figure 8. Kaplan-Meier survival curves according to combined status of S100A8+ TC and S100A8+ IC expression in invasive carcinoma. Among the four combined groups, only S100A8+ TC (-)/S100A8+ IC (-) group showed better disease-specific survival compared to other groups.

3.3. S100A8+ immune cells and other immune cell subsets

3.3.1. Association of S100A8+ immune cells with other immune cell subset infiltration

As MDSCs are known to be associated with regulatory T cell infiltration and PD-L1 induction, the correlation between S100A8+ IC, TIL subsets, and PD-L1+ IC infiltration was analyzed in pre-invasive and invasive carcinomas. In pre-invasive carcinoma, infiltration of S100A8+ IC revealed weak positive correlations with infiltration of CD4+, CD8+, and FOXP3+ TIL and PD-L1+ IC (rho, 0.209~0.281, **Table 10**). In invasive carcinoma, infiltration of S100A8+ IC showed a weak positive correlation with infiltration of CD4+ TIL (rho=0.263) and a moderate positive correlation with infiltration of CD8+ and FOXP3+ TIL, and PD-L1+ IC (rho=0.474, 0.482 and 0.525, **Table 10**).

Table 11 shows the distribution of CD4+, CD8+, and FOXP3+ TILs and the frequency of PD-L1+ IC in relation to S100A8+ IC. Generally, TIL infiltration was significantly higher in S100A8+ IC (+) group than in S100A8+IC (-) group in both pre-invasive and invasive carcinoma as a whole (all $p<0.01$). PD-L1+ IC was more frequently observed in S100A8+ IC (+) group compared to S100A8+ IC (-) group in both pre-invasive and invasive carcinomas ($p=0.006$, $p<0.001$, respectively). In subgroup analyses by HR status, HR-positive subgroup showed a similar pattern as the whole group in both pre-invasive and invasive carcinomas. In HR-negative subgroup, pre-invasive carcinoma did not show a difference in TIL subset and PD-L1+ IC infiltration in relation to S100A8+ IC, whereas invasive carcinoma revealed significant higher TIL (CD4+ TIL, $p=0.012$; CD8+ TIL, $p<0.001$; FOXP3+ TIL, $p<0.001$) and PD-L1+ IC infiltration ($p=0.004$) in S100A8+ IC (+) group compared to S100A8+ IC (-) group.

Table 10. Correlations between S100A8+ ICs, infiltration of CD4+, CD8+, and FOXP3+ TILs and PD-L1+ ICs in pre-invasive and invasive carcinoma

Disease group	Correlation between markers	S100A8+ IC	CD4+ TIL	CD8+ TIL	FOXP3+ TIL	PD-L1+ IC
Pre-invasive carcinoma	S100A8+ IC	-	0.281 (<0.001)	0.249 (0.001)	0.209 (0.006)	0.248 (0.001)
	CD4+ TIL	0.281 (<0.001)	-	0.610 (<0.001)	0.463 (<0.001)	0.391 (<0.001)
	CD8+ TIL	0.249 (0.001)	0.610 (<0.001)	-	0.458 (<0.001)	0.344 (<0.001)
	FOXP3+ TIL	0.209 (0.006)	0.463 (<0.001)	0.458 (<0.001)	-	0.434 (<0.001)
	PD-L1+ IC	0.248 (0.001)	0.391 (<0.001)	0.344 (<0.001)	0.434 (<0.001)	-
Invasive carcinoma	S100A8+ IC	-	0.263 (<0.001)	0.474 (<0.001)	0.482 (<0.001)	0.525 (<0.001)
	CD4+ TIL	0.263 (<0.001)	-	0.487 (<0.001)	0.306 (<0.001)	0.336 (<0.001)
	CD8+ TIL	0.474 (<0.001)	0.487 (<0.001)	-	0.588 (<0.001)	0.616 (<0.001)
	FOXP3+ TIL	0.482 (<0.001)	0.306 (<0.001)	0.588 (<0.001)	-	0.565 (<0.001)
	PD-L1+ IC	0.525 (<0.001)	0.336 (<0.001)	0.616 (<0.001)	0.565 (<0.001)	-

Data are presented as rho correlation coefficients calculated by Spearman's rank correlation test and *p* values in parentheses.

Table 11. Comparison of IC subset infiltration in relation to S100A8+ ICs

Immune cell subset	Pre-invasive carcinoma†		*p* value	Invasive carcinoma‡		*p* value
	S100A8+ IC (-)	S100A8+ IC (+)		S100A8+ IC (-)	S100A8+ IC (+)	
Total						
CD4+ TIL	15.33 (2.33-34.00)	35.00 (9.67-90.17)	<0.001	76.00 (30.50-136.50)	127.50 (52.50-195.50)	<0.001
CD8+ TIL	9.0 (4.33-19.33)	15.00 (8.83-41.33)	<0.001	59.00 (29.50-110.00)	166.00 (81.50-290.50)	<0.001
FOXP3+ TIL	0.00 (0.00-0.00)	0.00 (0.00-4.00)	0.006	5.00 (2.00-11.00)	17.00 (9.00-28.00)	<0.001
PD-L1+ IC	9/92 (9.8)	21/82 (25.6)	0.006	38/161 (23.6)	100/146 (68.5)	<0.001
HR+ subgroup						
CD4+ TIL	14.33 (2.00-29.33)	43.00 (9.33-91.33)	<0.001	76.50 (34.25-136.75)	109.50 (46.50-188.00)	0.023
CD8+ TIL	9.00 (4.33-17.83)	14.67 (9.00-39.00)	<0.001	56.00 (29.00-99.50)	133.00 (54.50-277.75)	<0.001
FOXP3+ TIL	0.00 (0.00-0.00)	0.00 (0.00-4.00)	0.012	5.00 (2.00-10.00)	15.00 (7.00-20.00)	<0.001
PD-L1+ IC	8/85 (9.4)	15/68 (22.1)	0.030	22/132 (16.7)	45/80 (56.3)	<0.001
HR- subgroup						
CD4+ TIL	53.3 (39.17-81.08)	27.67 (18.08-84.33)	0.689	71.00 (15.00-131.50)	138.50 (63.00-203.25)	0.012
CD8+ TIL	18.50 (6.08-38.92)	19.00 (6.58-65.50)	0.585	77.00 (35.00-163.00)	195.00 (108.50-306.50)	<0.001
FOXP3+ TIL	0.50 (0.00-5.92)	1.00 (0.00-5.75)	0.904	8.00 (3.00-11.50)	19.00 (12.00-33.25)	<0.001
PD-L1+ IC	1/7 (14.3)	6/14 (42.9)	0.337	16/29 (55.2)	55/66 (83.3)	0.004

P values are calculated by Mann-Whitney *U* test or Chi-square test. Data are presented as median (interquartile range) for TIL and frequency (%) for PD-L1+ IC.

†In pre-invasive carcinomas, data on immune cell subset infiltration was missing in six cases: CD4+ TIL in one case, FOXP3+ TI in two cases, CD8+ TIL in one case, and PD-L1+ IC in two cases.

‡In invasive carcinomas, data on immune cell subset infiltration was missing in three cases: CD8+TIL in one case, FOX3+ TIL in one case, and PD-L1+ IC in one case.

3.3.2. Combined effect of S100A8+ immune cells and other immune cell subset infiltration on clinical outcome

Besides S100A8+ IC, the presence of PD-L1+ IC was associated with ipsilateral breast recurrence in pre-invasive carcinoma (p=0.001). Low infiltration of CD8+ TIL and high infiltration of FOX3+ TIL tended to be associated with ipsilateral breast recurrence (p=0.111, p=0.103, respectively) while CD4+ TIL infiltration did not show an association with ipsilateral breast recurrence (p=0.421). In subgroup analyses, infiltration of S100A8+ ICs was associated with ipsilateral breast recurrence in the PD-L1+ IC (-), CD8+ TIL-low, and FOXP3+ TIL-low subgroups (p=0.017, p=0.042, p=0.040, respectively), but not in the PD-L1+ IC (+), CD8+ TIL-high, and FOXP3+ TIL-high subgroups (p=0.594, p=0.116, p=0.277, respectively) (**Figure 9**).

In invasive carcinoma, infiltration of CD4+, CD8+, and FOXP3+ TIL showed an association with disease-specific survival (p=0.015, p=0.039, p=0.069, respectively) albeit borderline significance for FOXP3+ TIL. The presence of PD-L1+ IC was not associated with patients' disease-specific survival (p=0.213). In subgroup analyses, infiltration of S100A8+ ICs was associated with decreased disease-specific survival in the PD-L1+ IC (-), CD8+ TIL-low, and FOXP3+ TIL-low subgroups (p=0.002, p=0.025, p=0.032, respectively), but not in the PD-L1+ IC (+), CD8+ TIL-high, and FOXP3+ TIL-high subgroups (p=0.503, p=0.949, p=0.248, respectively) (**Figure 10**).

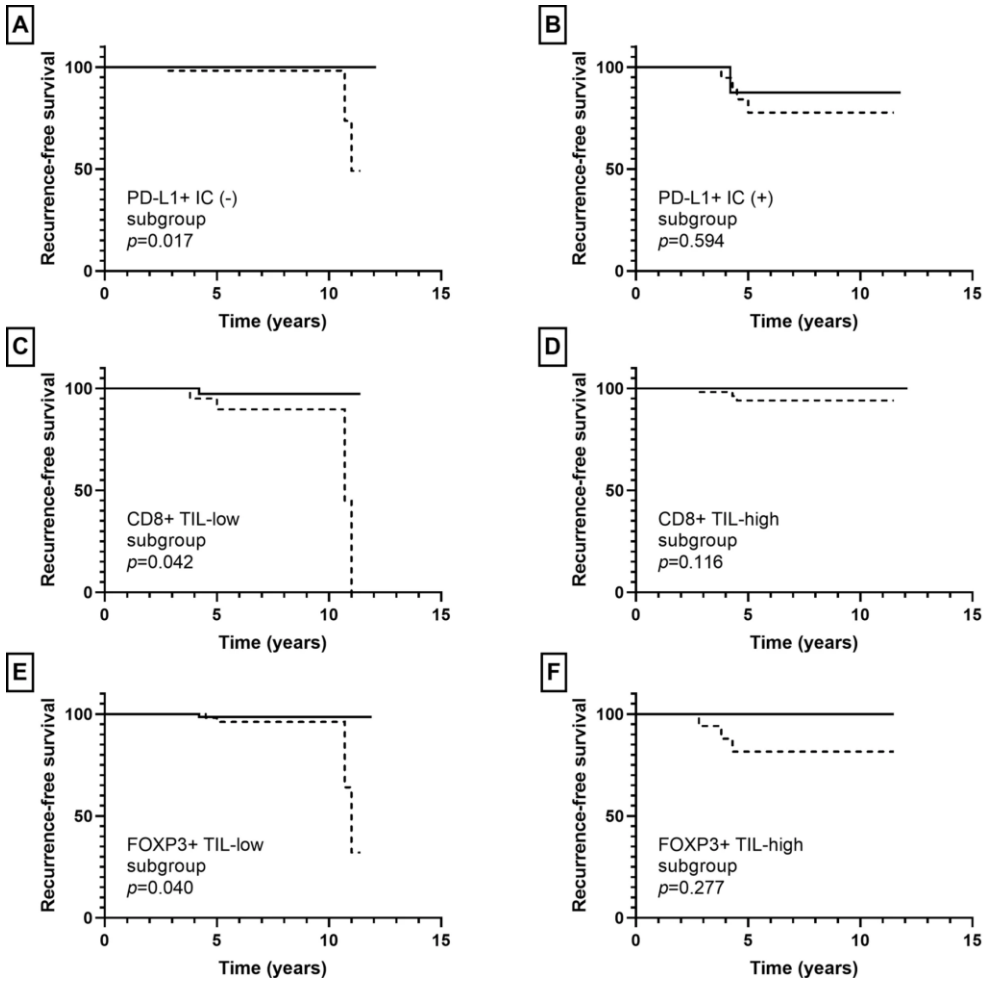

Figure 9. Kaplan-Meier survival curves according to combination of S100A8+ IC and other IC subset infiltration in pre-invasive carcinoma. Solid line indicates S100A8+ IC (-) group and dotted line indicates S100A8+ IC (+) group. **A, C, E** S100A8+ IC (+) group was associated with shorter ipsilateral breast cancer recurrence-free survival in subgroups of PD-L1+ IC (-), CD8+ TIL-low, FOXP3+ TIL-low (p=0.017, 0.042, 0.040, respectively). **B, D, F** No statistical difference in recurrence-free survival was observed regardless of S100A8+ IC status in subgroups of PD-L1+ IC (+), CD8+ TIL-high, FOXP3+ TIL-high.

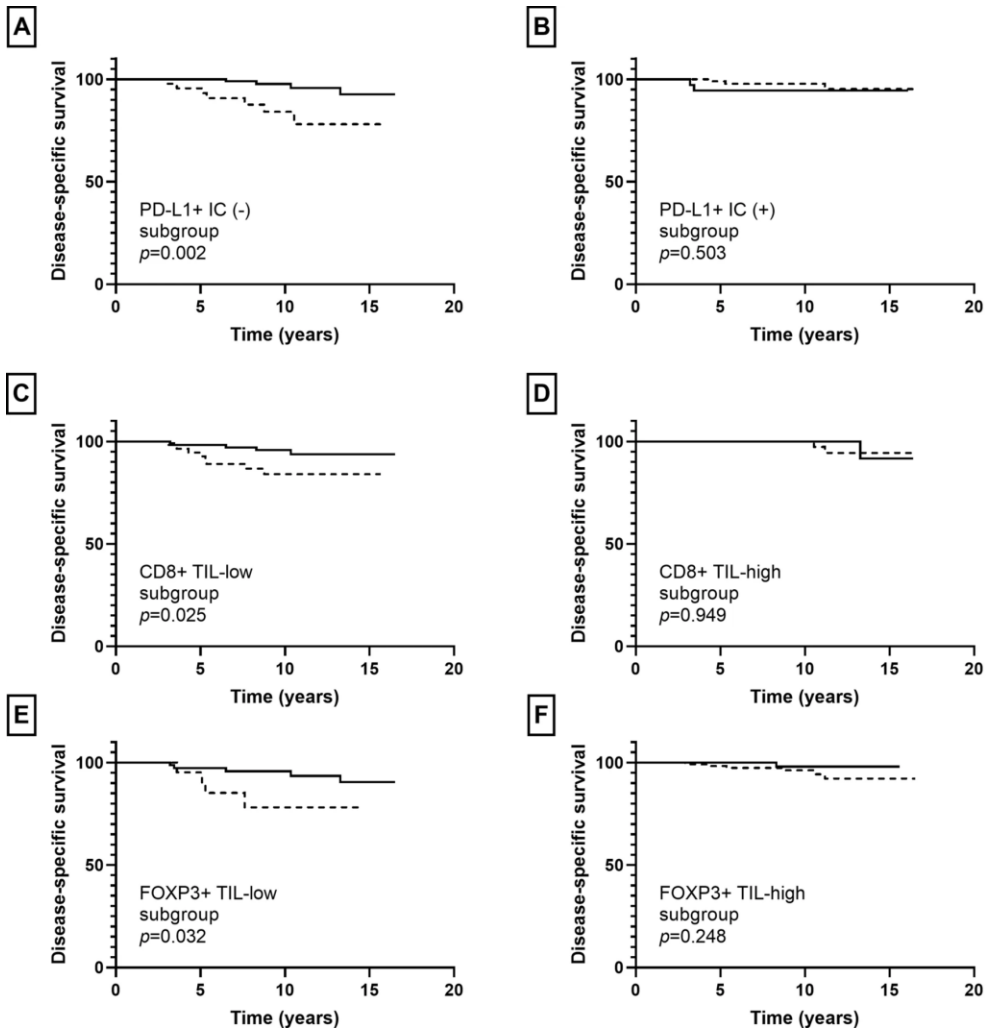

Figure 10. Kaplan-Meier survival curves according to combination of S100A8+ IC and other IC subset infiltration in invasive carcinoma. Solid line indicates S100A8+ IC (-) group and dotted line indicates S100A8+ IC (+) group. **A, C, E** S100A8+ IC (+) group showed poor disease-specific survival in the PD-L1+ IC (-), CD8+ TIL-low, FOXP3+ TIL-low subgroups (p=0.002, 0.025, 0.032, respectively). **B, D, F** No difference in disease-specific survival was observed regardless of S100A8+ IC status in PD-L1+ IC (+), CD8+ TIL-high, FOXP3+ TIL-high subgroups.

3.4. Evaluation of phenotype of S100A8+ immune cells

Figure 11 and **Figure 12** demonstrate S100A8, CD33, CD15 and CD163 IHC staining results in serial sections of representative HR-positive and HR-negative invasive breast carcinoma cases. In a HR-positive case (**Figure 11**), S100A8 was strongly stained in immune cells of peritumoral stroma. CD33, a classic myeloid marker, was weak but clearly expressed in the stromal immune cells. CD15, a PMN-MDSC marker which is expressed with CD33, was totally negative. CD163, known as M2-macrophage marker, was strongly stained in the stroma. In a HR-negative case (**Figure 12**), S100A8 was strongly stained in immune cells and some of the tumor cells. CD33 staining was weak but present in the stromal immune cells. CD15 was rarely stained except for a few scattered cells in the stroma. CD163 showed intense positivity and the staining pattern was similar to S100A8 and CD33.

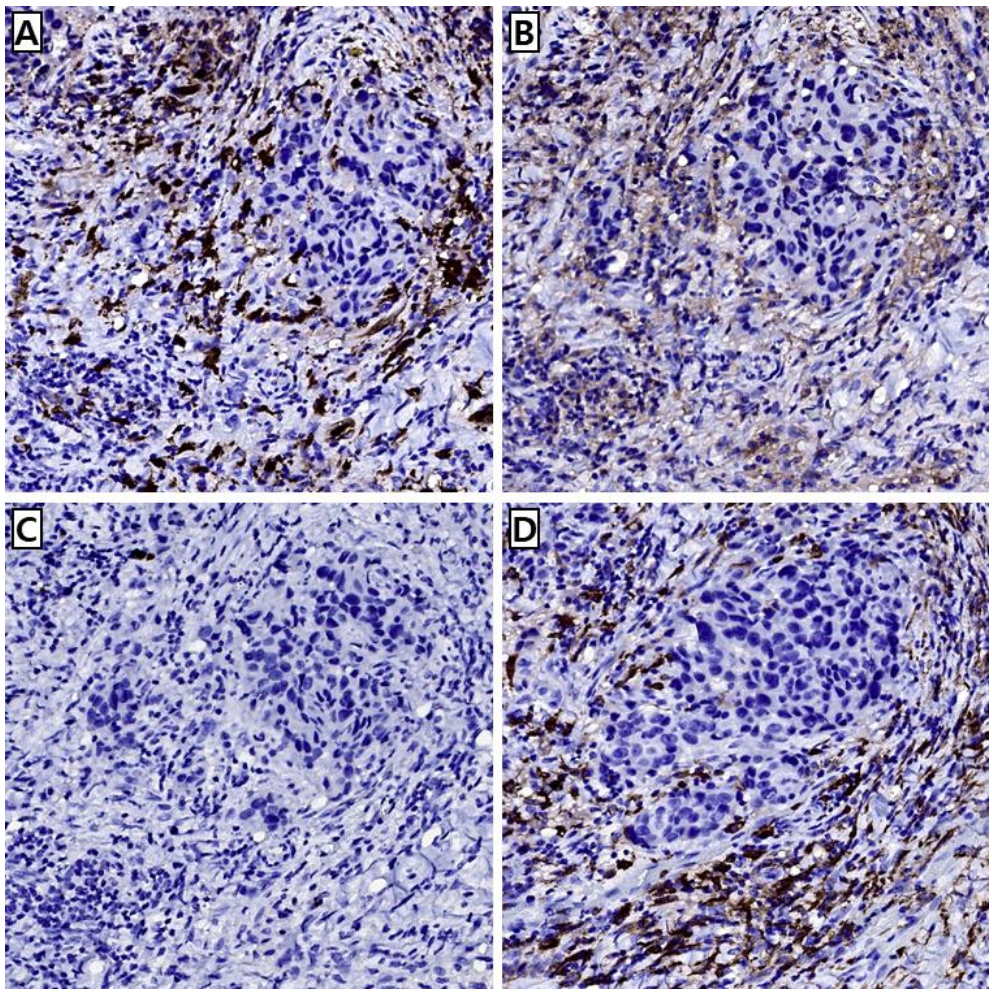

Figure 11. S100A8, CD33, CD15 and CD163 staining in serial sections of a representative HR-positive invasive carcinoma case. **A** Strong S100A8 staining was observed in peritumoral stroma. **B** Weak but widespread stain for CD33 was observed in the stroma. **C** CD15 was rarely stained and read as negative. **D** CD163 showed similar staining pattern like CD33 but was more intense.

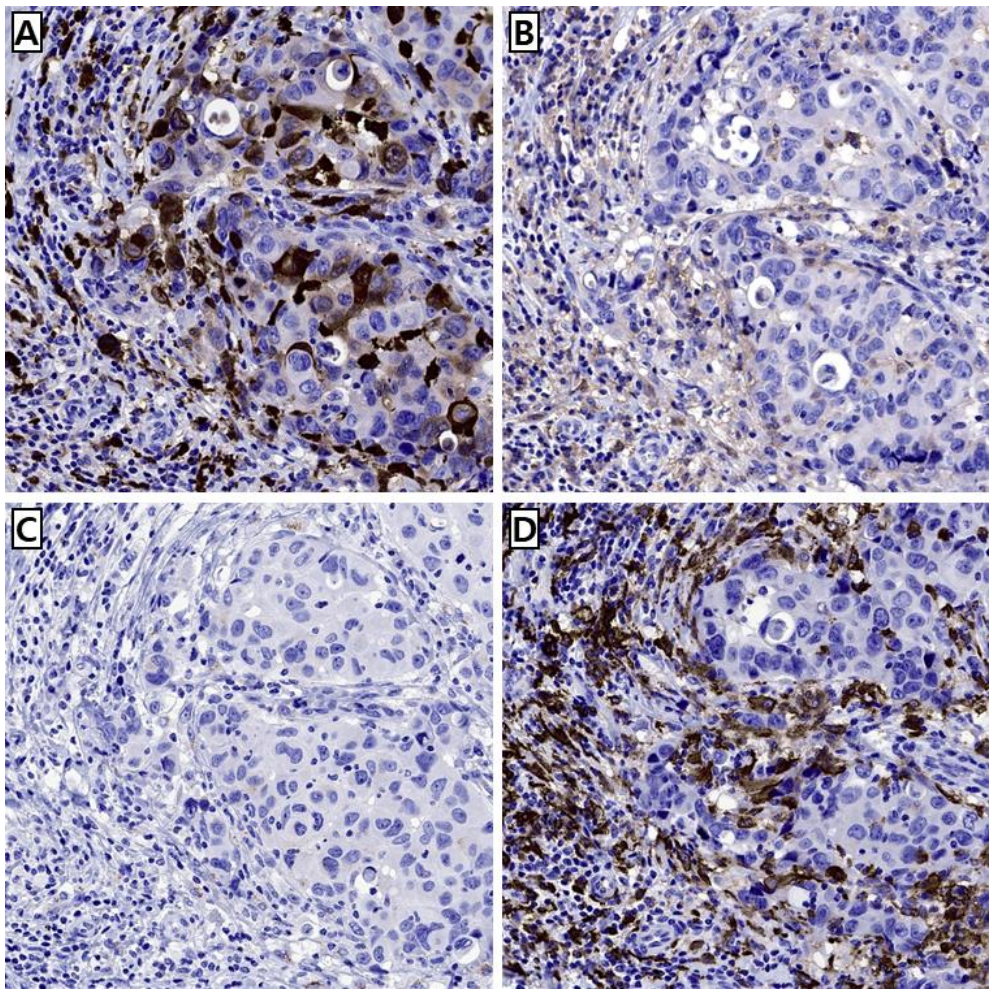

Figure 12. S100A8, CD33, CD15 and CD163 staining in serial sections of a representative HR-negative invasive carcinoma case. **A** S100A8 was strongly stained in immune cells and some of the tumor cells. **B** Weak CD33 staining was observed in stromal area. **C** A few CD15 positive cells were scattered in stroma. **D** CD163 showed similar staining pattern like CD33 but much more intense staining.

4. Discussion

Heatmaps drawn from immune profiling analysis showed a distinct pattern that could be largely grouped into three clusters. These clusters, however, does not seem to match with HR or HER2 status of the tumor. Tekpli et al. [6] analyzed immune profiling of 95 invasive breast cancer samples using the same method used in this study, nCounter PanCancer Immune Profiling array. They found three distinct immune clusters as well and named them cluster A, B, and C, which were independent of known clinicopathologic features such as HR or HER2 status. Lymphoid and myeloid infiltrations gradually increased from cluster A to B and C, making the immune contexture of the clusters immune cold and hot. These results are consistent with the current study and it is assumed that cluster A, B and C correspond with cluster 1, 2 and 3 of this study. Interestingly, in the cluster B with worst prognosis, higher level of M2 macrophages was found compared to cluster A and C. In the present study, S100A8 showed the largest fold change value in cluster 2 and S100A8+ ICs are thought to be macrophages derived from M-MDSCs (described in detail below). To sum up, distinct immune microenvironment possibly related to worse prognosis exists in breast cancer and it is independent of conventional biomarkers. S100A8 is an essential gene up-regulated in that condition and mostly expressed in macrophages derived from M-MDSCs.

Of note, the results of top 20 DEGs in the cluster 2 compared to other clusters were different in pre-invasive and invasive carcinoma. In pre-invasive carcinoma, although the sample size was more limited, none of the genes showed significant change in expression. This indirectly suggests that immune environment evolves during in situ to invasive transition. The results of top 20 DEGs by HR status, however, showed some common genes between pre-invasive and invasive carcinoma groups. It is expected that HR status affects the immune environment from early pre-invasive stage of the tumor but it isn’t the only factor that finally decides tumor immunity.

There were some common DEGs in the cluster 2 and HR-negative invasive carcinoma as well as in the HR-negative pre-invasive and invasive carcinoma. Some of the genes were related to tumor-associated macrophages (TAMs) or MDSCs. CCL5 promotes breast cancer recurrence by recruiting CCR5-expressing macrophages [27]. CX3CL1 is a pro-tumor chemokine acting as a key recruiter of TAMs [28]. CXCL1 is the most abundant chemokine secreted by TAMs that can promote breast cancer migration and invasion [29]. CCL5-CCR5 axis is a major regulator of immunosuppressive myeloid cells and its absence abrogated the generation of MDSCs [30]. Cancer progression was exacerbated in mice with stroke by increasing LCN2 expression in PMN-MDSCs [31]. Among the DEGs, S100A8 was finally selected for further analysis as it showed the most striking fold change value and matched with our interest in MDSCs.

Originally, S100A8 was known as a pro-inflammatory danger signal expressed by myeloid origin cells (neutrophil, macrophage and monocyte) in an inflammatory environment, but recent studies have focused on the relationship between MDSCs and S100A8 in tumors [32]. As the phenotypic complexity of MDSCs complicates various analyses, surrogate markers of MDSCs have been developed, and one of the well-known marker for MDSC is S100A8 [15]. MDSCs are largely divided into two categories: M-MDSCs and PMN-MDSCs. In human cancer, M-MDSCs rather than PMN-MDSCs seem to be the major source of S100A8 although studies on S100A8 production by MDSC subsets have shown great variations by cancer type [32]. S100A8 forms a stable protein complex with S100A9 and works as a heterodimer of S100A8/A9 known as calprotectin. It generates and recruits MDSCs, and supports an autocrine feedback loop that sustains accumulation of MDSCs in a tumor [33, 34]. S100A8 is known to promote tumor proliferation and migration, and it even forms pre-metastatic niches [35-37].

Staining result of S100A8 IHC was consistent with the DEGs in NanoString nCounter analyses according to HR status and overexpression of

S100A8 in HR-negative breast cancers was validated in tissue microarray. S100A8 was expressed in ICs and TCs. Next, S100A8 expression was compared in pre-invasive and invasive carcinoma of the breast and significant higher infiltration of S100A8+ ICs was observed in invasive carcinoma than pre-invasive carcinoma. Many studies on circulating MDSCs have reported that MDSCs accumulate systemically in the body from the pre-invasive stage and exerts the same immunosuppressive role as they do in various cancers including the breast [25, 38-40]. Particularly, Clark et al. [38] revealed that circulating MDSCs progressively accumulate from normal to pre-invasive to invasive pancreatic cancer. Put together, it can be deduced that MDSCs already exist in a pre-invasive tumor and increase in number as the tumor progresses. Additionally, the difference in S100A8+ IC infiltration between pre-invasive and invasive carcinomas was evident in HR-negative tumors, but not in HR-positive tumors. However, as the number of HR-negative pre-invasive carcinoma was quite small (n=21), and many HR-positive tumors showed no S100A8+ IC infiltration, further large-series study is warranted to confirm this finding.

In contrast to S100A8+ IC infiltration, the presence of S100A8+ TCs did not differ between pre-invasive and invasive carcinomas. Expression of S100A8 in invasive breast carcinoma has been studied using immunohistochemistry [19, 41-44]. Previously, Arai et al. [41] reported that S100A8 expression was found in 66.7% (16/24) of ductal carcinoma in situ (DCIS) and 45.5% (46/101) of invasive ductal carcinoma with a slightly higher frequency in DCIS. In our study, in terms of frequency of positive cases, S100A8+ TCs was found in 30.7% (54/176) of pre-invasive carcinomas and 33.4% (175/524) of invasive carcinomas without a statistical difference (data not shown). Similarly, Choi et al. [44] have reported no difference in S100A8 expression in TCs between primary invasive ductal carcinoma and adjacent DCIS. In addition, it was shown that S100A8 expression in TCs was associated with poor clinicopathologic features in both pre-invasive and

invasive carcinomas as reported in previous studies [19, 41-44]. Thus, it seems that S100A8 is expressed in TCs of pre-invasive carcinoma just as much as invasive carcinoma in association with aggressive clinicopathologic features of tumor.

In survival analyses, infiltration of S100A8+ ICs was associated with ipsilateral breast recurrence in pre-invasive carcinoma, and it was found to be an independent poor prognostic factor in invasive carcinoma. These results suggest that S100A8+ ICs play an important role during progression of both pre-invasive and invasive carcinomas. Thus, pre-invasive and invasive breast carcinomas with high S100A8+ IC infiltration could be a target for close observation and aggressive additional treatment. Additionally, in this study, decreased survival was evident in HR-positive subgroup, but not in HR-negative subgroup. Miller et al. [42] demonstrated a clear difference in overall survival according to S100A8 expression in both HR-positive and negative subgroups using automated quantitative immunofluorescence. This discrepancy in results seems to be from the difference in evaluation method since they used different cutoffs for HR-positive and negative tumors and the method could read the intensity of S100A8 expression. Even though applying different cutoffs was tried in HR-negative tumors, similar results were obtained in this study (data not shown).

When combining the status of S100A8+ TCs and ICs, interesting survival curves were drawn. Patients in S100A8+ TC (-)/S100A8+ IC (+) group steadily deceased from the disease and eventually showed same survival rate as S100A8+ TC (+) group after more than 10 years. This phenomenon reminds of the dormancy of breast cancer. Subtype distribution of this group was diverse as follows: 50 cases (27.3%) of luminal A, 60 cases (32.8%) of luminal B, 25 cases of HER2+ (13.7%), and 48 cases (26.2%) of TNBC. Tumor dormancy and reactivation is one of the mysterious field of research. Clinically undetectable disseminated tumor cells must escape from the immune surveillance system while they are at their dormant stage and MDSCs are considered as a major player of tumor release from dormancy [45].

Perego et al. [46] found in their dormancy mouse models of lung and ovarian cancer that reactivation of dormant cells was dependent on higher serum concentrations of S100A8/A9 by stress-induced release from neutrophils. While it is premature to tell the role of S100A8 in tumor dormancy due to scarcity of evidence, it is a promising avenue for future research.

There have been no studies on the correlation between S100A8+ ICs and TIL subsets or PD-L1+ ICs though the possible close relationship is expected considering various immunomodulatory functions of S100A8 protein. Investigation was done about the relationship between S100A8+ ICs and other TIL subsets infiltration including CD4+, CD8+, and FOXP3+ TILs and PD-L1+ ICs as well as the prognostic significance of S100A8+ ICs in various immune environments. In combined analyses of S100A8+ IC and other IC subset infiltration, infiltration of S100A8+ IC was associated with decreased disease-specific survival in the PD-L1+ IC (-), CD8+ TIL-low, and FOXP3+ TIL-low subgroups in invasive carcinomas. Similarly, infiltration of S100A8+ IC was associated with decreased ipsilateral breast recurrence-free survival in the same subgroups in pre-invasive carcinomas. That is, the prognostic significance of S100A8+ ICs was more prominent in less immunogenic tumors. Thus, it can be postulated that S100A8+ ICs could play a role in tumor progression via a non-immune mechanism, such as neovascularization and promotion of epithelial-mesenchymal transition rather than immune-mediated mechanism. In line with our results, Drews-Elger et al. [37] demonstrated that recruitment of S100A8+ myeloid cells in xenograft models of breast cancer enhance tumor progression independent of their suppressive activity on T cells using immunosuppressed mouse models. This is the first study that showed the positive relationship between S100A8+ ICs and various IC subsets and analyzed their combined prognostic impact using human breast cancer tissues. Further investigation is needed to elucidate our findings.

S100A8+ ICs showed a weak to moderate positive correlation with other

IC subset infiltration, and CD4+, CD8+, FOXP3+ TIL and PD-L1+ IC infiltration was significantly higher in S100A8+ IC (+) group compared to S100A8+ IC (-) group. The positive correlation between S100A8+ ICs and other IC subset was more prominent in invasive carcinoma than in pre-invasive carcinoma. Changes in other immune cell subsets can be explained by immune-suppressive functions of MDSCs, though it is cautious because S100A8+ ICs may not harbor all the characteristics of MDSCs. MDSCs induce regulatory T cells [47-49] and FOXP3+ TIL infiltration increased in S100A8+ IC (+) group. Tumor-infiltrating MDSCs show upregulated expression of PD-L1 [50] and PD-L1+ ICs were increased in S100A8+ IC (+) group. CD8+ TIL, known for its anti-tumor activity, also showed a positive correlation with S100A8+ IC infiltration in pre-invasive and invasive carcinomas. However, the anti-tumor activity of CD8+ TILs in S100A8+ ICs (+) group remains unclear since interference by MDSCs can result in CD8+ T cell tolerance [51-53].

The important and essential question, if S100A8-stained ICs could be called as authentic MDSCs, needs to be answered. Defining phenotype of MDSCs in human tissue is complex but CD33, CD15 and CD163 were adopted referring to previous articles [15, 25, 26] and in terms of availability. Ma et al. [25] summarized MDSC subpopulation as follows: Total MDSC (CD11b+ HLA-DR-/low), PMN-MDSC (CD11b+ HLA-DR-/low CD15+ CD14-) and M-MDSC (CD11b+ HLA-DR-/low CD15- CD14+). Bronte et al. [15] mentioned that CD33 myeloid marker can be used instead of CD11b since very few CD15+ cells are CD11b-. It was also reported that M-MDSCs express the myeloid marker CD33, whereas PMN-MDSCs display $CD33^{dim}$ staining [54]. CD163 was added to see the degree of differentiation to macrophage in this study. Before staining, it was assumed that most of the S100A8+ ICs are M-MDSCs and the results of staining were expected as CD33+ CD15- and CD163+/- depending on the M-MDSC maturity because M-MDSCs are the major source of S100A8 in human as

mentioned above [32] and most of the observed S100A8+ ICs were spindled, macrophage-looking cells.

Serial IHC staining on representative cases showed that most of the S100A8+ ICs were CD33+ CD15- CD163+ cells. Recently, Kwak et al. [26] reported that macrophages differentiated from M-MDSCs, in contrast to macrophages differentiated from monocytes, are immune-suppressive and their immune-suppressive function is dependent on the persistent expression of S100A8/A9 protein. Taken together, the majority of S100A8+ ICs can be called macrophages differentiated from M-MDSCs with their immunosuppressive function preserved.

Pivotal role of S100A8 in disease development was not only demonstrated in cancer but also in many inflammatory diseases such as systemic lupus erythematosus or inflammatory bowel disease. Pruenster et al. [55] summarized the biologic function of S100A8/A9 and gave an outlook in terms of diagnostic and therapeutic application targeting S100A8/A9 in their review article. Monitoring S100A8/A9 concentrations in serum or disease specific sites such as joints or feces has proved its benefit as a biomarker of disease activity in various inflammatory conditions. Application of S100A8 as a diagnostic marker for cancer progression would be promising and needs to be investigated. However, targeting the molecule for therapeutic purposes has not been successful in human yet. Phase III study of Eritoran [56], a synthetic lipid A antagonist that blocks lipopolysaccharide from binding at the cell surface MD2-TLR4 receptor, did not reduced mortality in patients with severe sepsis compared with placebo. Deguchi et al. [57] later used Eritoran to treat Lewis lung carcinoma-bearing mice. In the report, they showed S100A8 stimulated tumor migration in a manner dependent on TLR4/MD-2 and introduced Eritoran as a S100A8 blocking agent. Tumor volume and pulmonary recruitment of MDSCs were reduced with the treatment of Eritoran. Future clinical trials would be worth especially for cancer patients with high S100A8+ ICs.

There are several limitations in this study. First, S100A8 expression was read manually and TMAs were used instead of evaluating whole sections. Several countermeasures were adopted to minimize the limitation: setting strict reading criteria, categorization of continuous values, and use of multiple TMA cores. Second, the intensity of S100A8 staining was not considered when reading TMAs as mentioned above. Lastly, caution should be exercised when interpreting the results of S100A8+ ICs. Though S100A8 is a surrogate marker of MDSCs, most of the S100A8+ ICs observed in this study are thought to be M-MDSC derived macrophages. Both cells harbor immune-suppressive function but it cannot be assured that M-MDSC derived macrophages have all the reported functions of MDSCs. Plus, the phenotype of MDSCs is still complex and vague, especially in human tissue. However, movements of defining phenotype of MDSCs were made lately [15]. Further studies are warranted to elucidate the exact role of S100A8+ ICs in immune microenvironment and their utilization in cancer therapeutics.

5. Conclusion

In summary, NanoString nCounter immune profiling analysis revealed some DEGs according to unsupervised clustering and HR status. Among them, S100A8, which is well known for a surrogate marker of MDSCs, was selected for its highest difference in expression. S100A8 was expressed in both TCs and ICs in breast cancer samples by IHC. Differential expression was validated in TMAs according to HR status. Infiltration of S100A8+ ICs was associated with aggressive clinicopathological features and poor clinical outcome in breast cancer patients. S100A8+ ICs were already present in early stage of breast cancer and were associated with increased CD4+, CD8+ and FOXP3+ TIL and PD-L1+ IC infiltration. In combined survival analyses, prognostic impact of S100A8+ ICs was stronger in HR-positive, PD-L1+ IC (-), CD8+ TIL-low and FOXP3+ TIL-low subgroups, which are characterized as less immunogenic tumors. S100A8+ ICs are assumed as macrophages differentiated from M-MDSCs because the majority of S100A8+ ICs showed CD33+ CD15- CD163+ phenotype. Further investigation on therapeutic intervention targeting S100A8 is warranted.

Supplementary Tables

Supplementary Table 1. Baseline characteristics of pre-invasive carcinomas for NanoString nCounter assay

Characteristic	No. (n=16)
Age at diagnosis, years	
Median	52.2
Range	35.8-76.8
Extent, cm	
Median	4.0
Range	1.7-9.0
Nuclear grade	
Low	0 (0.0)
Intermediate	6 (37.5)
High	10 (62.5)
Comedo-type necrosis	
Absent	8 (50.0)
Present	8 (50.0)
Estrogen receptor	
Positive	8 (50.0)
Negative	8 (50.0)
Progesterone receptor	
Positive	8 (50.0)
Negative	8 (50.0)
HER2 status	
Negative	10 (62.5)
Positive	6 (37.5)
Ki67 index	
Low (<10%)	5 (31.3)
High (≥10%)	11 (68.8)
P53 overexpression	
Absent	8 (50.0)
Present	8 (50.0)
Subtype	
Luminal A	5 (31.3)
Luminal B	3 (18.8)
HER2+	6 (37.5)
Triple negative	2 (12.5)

Supplementary Table 2. Baseline characteristics of invasive carcinomas for NanoString nCounter assay

Characteristic	No. (n=32)
Age at diagnosis, years	
Median	49.7
Range	35.1-78.6
pT stage	
pT1	10 (31.3)
pT2	21 (65.6)
pT3	1 (3.1)
pN stage*	
pN0	13 (40.6)
pN1	10 (31.3)
pN2	5 (15.6)
pN3	3 (9.4)
Histologic subtype	
Invasive carcinoma of no special type	32 (100.0)
Histologic grade	
I	2 (6.3)
II	3 (9.4)
III	27 (84.4)
Lymphovascular invasion	
Absent	10 (31.3)
Present	22 (68.8)
Estrogen receptor	
Positive	16 (50.0)
Negative	16 (50.0)
Progesterone receptor	
Positive	15 (46.9)
Negative	17 (53.1)
HER2 status	
Negative	19 (59.4)
Positive	13 (40.6)
Ki-67 proliferation index	
<20%	11 (34.4)
≥20%	21 (65.6)
P53 overexpression	
Absent	19 (59.4)
Present	13 (40.6)
Subtype	
Luminal A	6 (18.8)
Luminal B	10 (31.3)
HER2 positive	13 (40.6)
Triple negative	3 (9.4)

* Data is missing in one case

Supplementary Table 3. Baseline characteristics of pre-invasive carcinomas for tissue microarray

Characteristic	No. (n=176)
Age at diagnosis, years	
Mean ± standard deviation	48.3 ± 10.0
Follow-up, years	
Mean ± standard deviation	6.7 ± 3.0
Extent, cm	
Mean ± standard deviation	3.2 ± 2.1
Histologic subtype	
Ductal carcinoma in situ	175 (99.4)
Mixed ductal and lobular carcinoma in situ	1 (0.6)
Nuclear grade	
Low	11 (6.3)
Intermediate	98 (55.7)
High	67 (38.1)
Comedo-type necrosis	
Absent	133 (75.6)
Present	43 (24.4)
Estrogen receptor	
Positive	154 (87.5)
Negative	22 (12.5)
Progesterone receptor	
Positive	134 (76.1)
Negative	83 (23.9)
HER2 status	
Negative	151 (85.8)
Positive	25 (14.2)
Ki67 index	
Low (<10%)	165 (93.8)
High (≥10%)	11 (6.3)
P53 overexpression	
Absent	155 (88.1)
Present	21 (11.9)
Subtype	
Luminal A	127 (72.2)
Luminal B	28 (15.9)
HER2+	8 (4.5)
Triple negative	13 (7.4)
Adjuvant radiation therapy	
Not received	71 (40.3)
Received	105 (59.7)
Adjuvant hormonal therapy	
Not received	105 (59.7)
Received	71 (40.3)

Supplementary Table 4. Baseline characteristics of invasive carcinomas for tissue microarray

Characteristic	No. (n=524)
Age at diagnosis, years	
Mean ± standard deviation	51.2 ± 11.8
Follow up, years	
Mean ± standard deviation	9.4 ± 4.0
pT stage	
pT1	246 (47.0)
pT2	251 (47.9)
pT3	19 (3.6)
pT4	8 (1.5)
pN stage	
pN0	300 (57.3)
pN1	137 (26.1)
pN2	50 (9.5)
pN3	37 (7.1)
Histologic subtype	
Invasive carcinoma of no special type	456 (87.0)
Invasive lobular carcinoma	20 (3.8)
Mucinous carcinoma	15 (2.9)
Metaplastic carcinoma	14 (2.7)
Others	19 (3.6)
Histologic grade	
I	94 (17.9)
II	166 (31.7)
III	264 (50.4)
Lymphovascular invasion	
Absent	296 (56.5)
Present	228 (43.5)
Estrogen receptor	
Positive	353 (67.4)
Negative	171 (32.6)
Progesterone receptor	
Positive	278 (53.1)
Negative	246 (46.9)
HER2 status	
Negative	404 (77.1)
Positive	120 (22.9)
Ki-67 proliferation index	
<20%	301 (57.4)
≥20%	223 (42.6)
P53 overexpression	
Absent	386 (73.7)
Present	138 (26.3)

Bibliography

1. Sung, H., et al., *Global Cancer Statistics 2020: GLOBOCAN Estimates of Incidence and Mortality Worldwide for 36 Cancers in 185 Countries.* CA Cancer J Clin, 2021. **71**(3): p. 209-249.
2. Kang, S.Y., et al., *Breast Cancer Statistics in Korea in 2017: Data from a Breast Cancer Registry.* J Breast Cancer, 2020. **23**(2): p. 115-128.
3. Waks, A.G. and E.P. Winer, *Breast Cancer Treatment: A Review.* JAMA, 2019. **321**(3): p. 288-300.
4. O'Meara, T., et al., *Immunological Differences Between Immune-Rich Estrogen Receptor-Positive and Immune-Rich Triple-Negative Breast Cancers.* JCO Precis Oncol, 2020. **4**.
5. Sadeghalvad, M., H.R. Mohammadi-Motlagh, and N. Rezaei, *Immune microenvironment in different molecular subtypes of ductal breast carcinoma.* Breast Cancer Res Treat, 2021. **185**(2): p. 261-279.
6. Tekpli, X., et al., *An independent poor-prognosis subtype of breast cancer defined by a distinct tumor immune microenvironment.* Nat Commun, 2019. **10**(1): p. 5499.
7. Trinh, A., et al., *Genomic Alterations during the In Situ to Invasive Ductal Breast Carcinoma Transition Shaped by the Immune System.* Mol Cancer Res, 2021. **19**(4): p. 623-635.
8. Wang, M., et al., *Mechanism of immune evasion in breast cancer.* Onco Targets Ther, 2017. **10**: p. 1561-1573.
9. Gabrilovich, D.I., S. Ostrand-Rosenberg, and V. Bronte, *Coordinated regulation of myeloid cells by tumours.* Nat Rev Immunol, 2012. **12**(4): p. 253-68.
10. Kumar, V., et al., *The Nature of Myeloid-Derived Suppressor Cells in the Tumor Microenvironment.* Trends Immunol, 2016. **37**(3): p. 208-220.
11. Weber, R., et al., *Myeloid-Derived Suppressor Cells Hinder the Anti-Cancer Activity of Immune Checkpoint Inhibitors.* Front Immunol, 2018. **9**: p. 1310.
12. Tartour, E., et al., *Angiogenesis and immunity: a bidirectional link potentially relevant for the monitoring of antiangiogenic therapy and the development of novel therapeutic combination with immunotherapy.* Cancer Metastasis Rev, 2011. **30**(1): p. 83-95.

13. Safari, E., et al., *Myeloid-derived suppressor cells and tumor: Current knowledge and future perspectives.* J Cell Physiol, 2019. **234**(7): p. 9966-9981.
14. Umansky, V., et al., *The Role of Myeloid-Derived Suppressor Cells (MDSC) in Cancer Progression.* Vaccines (Basel), 2016. **4**(4).
15. Bronte, V., et al., *Recommendations for myeloid-derived suppressor cell nomenclature and characterization standards.* Nat Commun, 2016. **7**: p. 12150.
16. Talla, S.B., et al., *Immuno-oncology gene expression profiling of formalin-fixed and paraffin-embedded clear cell renal cell carcinoma: Performance comparison of the NanoString nCounter technology with targeted RNA sequencing.* Genes Chromosomes Cancer, 2020. **59**(7): p. 406-416.
17. Prabhu, J.S., et al., *A Majority of Low (1-10%) ER Positive Breast Cancers Behave Like Hormone Receptor Negative Tumors.* J Cancer, 2014. **5**(2): p. 156-65.
18. Goldhirsch, A., et al., *Strategies for subtypes--dealing with the diversity of breast cancer: highlights of the St. Gallen International Expert Consensus on the Primary Therapy of Early Breast Cancer 2011.* Ann Oncol, 2011. **22**(8): p. 1736-47.
19. Bergenfelz, C., et al., *S100A9 expressed in ER(-)PgR(-) breast cancers induces inflammatory cytokines and is associated with an impaired overall survival.* Br J Cancer, 2015. **113**(8): p. 1234-43.
20. Vennapusa, B., et al., *Development of a PD-L1 Complementary Diagnostic Immunohistochemistry Assay (SP142) for Atezolizumab.* Appl Immunohistochem Mol Morphol, 2019. **27**(2): p. 92-100.
21. Dieci, M.V., et al., *Update on tumor-infiltrating lymphocytes (TILs) in breast cancer, including recommendations to assess TILs in residual disease after neoadjuvant therapy and in carcinoma in situ: A report of the International Immuno-Oncology Biomarker Working Group on Breast Cancer.* Semin Cancer Biol, 2018. **52**(Pt 2): p. 16-25.
22. Hendry, S., et al., *Assessing Tumor-Infiltrating Lymphocytes in Solid Tumors: A Practical Review for Pathologists and Proposal for a Standardized Method from the International Immuno-Oncology Biomarkers Working Group: Part 2: TILs in Melanoma, Gastrointestinal*

Tract Carcinomas, Non-Small Cell Lung Carcinoma and Mesothelioma, Endometrial and Ovarian Carcinomas, Squamous Cell Carcinoma of the Head and Neck, Genitourinary Carcinomas, and Primary Brain Tumors. Adv Anat Pathol, 2017. **24**(6): p. 311-335.

23. Chung, Y.R., et al., *Prognostic value of tumor infiltrating lymphocyte subsets in breast cancer depends on hormone receptor status.* Breast Cancer Res Treat, 2017. **161**(3): p. 409-420.
24. Kim, M., et al., *Immune microenvironment in ductal carcinoma in situ: a comparison with invasive carcinoma of the breast.* Breast Cancer Res, 2020. **22**(1): p. 32.
25. Ma, P., et al., *Circulating Myeloid Derived Suppressor Cells (MDSC) That Accumulate in Premalignancy Share Phenotypic and Functional Characteristics With MDSC in Cancer.* Front Immunol, 2019. **10**: p. 1401.
26. Kwak, T., et al., *Distinct Populations of Immune-Suppressive Macrophages Differentiate from Monocytic Myeloid-Derived Suppressor Cells in Cancer.* Cell Rep, 2020. **33**(13): p. 108571.
27. Walens, A., et al., *CCL5 promotes breast cancer recurrence through macrophage recruitment in residual tumors.* Elife, 2019. **8**.
28. Conroy, M.J. and J. Lysaght, *CX3CL1 Signaling in the Tumor Microenvironment.* Adv Exp Med Biol, 2020. **1231**: p. 1-12.
29. Wang, N., et al., *CXCL1 derived from tumor-associated macrophages promotes breast cancer metastasis via activating NF-kappaB/SOX4 signaling.* Cell Death Dis, 2018. **9**(9): p. 880.
30. Ban, Y., et al., *Targeting Autocrine CCL5-CCR5 Axis Reprograms Immunosuppressive Myeloid Cells and Reinvigorates Antitumor Immunity.* Cancer Res, 2017. **77**(11): p. 2857-2868.
31. Huang, T., et al., *Stroke Exacerbates Cancer Progression by Upregulating LCN2 in PMN-MDSC.* Front Immunol, 2020. **11**: p. 299.
32. Zheng, R., S. Chen, and S. Chen, *Correlation between myeloid-derived suppressor cells and S100A8/A9 in tumor and autoimmune diseases.* Int Immunopharmacol, 2015. **29**(2): p. 919-925.
33. Cheng, P., et al., *Inhibition of dendritic cell differentiation and accumulation of myeloid-derived suppressor cells in cancer is regulated by S100A9 protein.* J Exp Med, 2008. **205**(10): p. 2235-49.
34. Srikrishna, G., *S100A8 and S100A9: new insights into their roles in*

malignancy. J Innate Immun, 2012. **4**(1): p. 31-40.

35. Eisenblaetter, M., et al., *Visualization of Tumor-Immune Interaction - Target-Specific Imaging of S100A8/A9 Reveals Pre-Metastatic Niche Establishment.* Theranostics, 2017. **7**(9): p. 2392-2401.
36. Yin, C., et al., *RAGE-binding S100A8/A9 promotes the migration and invasion of human breast cancer cells through actin polymerization and epithelial-mesenchymal transition.* Breast Cancer Res Treat, 2013. **142**(2): p. 297-309.
37. Drews-Elger, K., et al., *Infiltrating S100A8+ myeloid cells promote metastatic spread of human breast cancer and predict poor clinical outcome.* Breast Cancer Res Treat, 2014. **148**(1): p. 41-59.
38. Clark, C.E., et al., *Dynamics of the immune reaction to pancreatic cancer from inception to invasion.* Cancer Res, 2007. **67**(19): p. 9518-27.
39. Allen, M.D. and L.J. Jones, *The role of inflammation in progression of breast cancer: Friend or foe? (Review).* Int J Oncol, 2015. **47**(3): p. 797-805.
40. Safarzadeh, E., et al., *Circulating myeloid-derived suppressor cells: An independent prognostic factor in patients with breast cancer.* J Cell Physiol, 2019. **234**(4): p. 3515-3525.
41. Arai, K., et al., *S100A8 and S100A9 overexpression is associated with poor pathological parameters in invasive ductal carcinoma of the breast.* Curr Cancer Drug Targets, 2008. **8**(4): p. 243-52.
42. Miller, P., et al., *Elevated S100A8 protein expression in breast cancer cells and breast tumor stroma is prognostic of poor disease outcome.* Breast Cancer Res Treat, 2017. **166**(1): p. 85-94.
43. Wang, D., et al., *Clinical Significance of Elevated S100A8 Expression in Breast Cancer Patients.* Front Oncol, 2018. **8**: p. 496.
44. Choi, J., et al., *Hornerin Is Involved in Breast Cancer Progression.* J Breast Cancer, 2016. **19**(2): p. 142-7.
45. Khadge, S., K. Cole, and J.E. Talmadge, *Myeloid derived suppressor cells and the release of micro-metastases from dormancy.* Clin Exp Metastasis, 2021. **38**(3): p. 279-293.
46. Perego, M., et al., *Reactivation of dormant tumor cells by modified lipids derived from stress-activated neutrophils.* Sci Transl Med, 2020. **12**(572).
47. Nagaraj, S. and D.I. Gabrilovich, *Regulation of suppressive function of*

myeloid-derived suppressor cells by CD4+ T cells. Semin Cancer Biol, 2012. **22**(4): p. 282-8.

48. Pan, P.Y., et al., *Immune stimulatory receptor CD40 is required for T-cell suppression and T regulatory cell activation mediated by myeloid-derived suppressor cells in cancer.* Cancer Res, 2010. **70**(1): p. 99-108.
49. Schlecker, E., et al., *Tumor-infiltrating monocytic myeloid-derived suppressor cells mediate CCR5-dependent recruitment of regulatory T cells favoring tumor growth.* J Immunol, 2012. **189**(12): p. 5602-11.
50. Lu, C., et al., *The expression profiles and regulation of PD-L1 in tumor-induced myeloid-derived suppressor cells.* Oncoimmunology, 2016. **5**(12): p. e1247135.
51. Nagaraj, S., et al., *Mechanism of T cell tolerance induced by myeloid-derived suppressor cells.* J Immunol, 2010. **184**(6): p. 3106-16.
52. Tran Janco, J.M., et al., *Tumor-infiltrating dendritic cells in cancer pathogenesis.* J Immunol, 2015. **194**(7): p. 2985-91.
53. Lesokhin, A.M., et al., *Monocytic CCR2(+) myeloid-derived suppressor cells promote immune escape by limiting activated CD8 T-cell infiltration into the tumor microenvironment.* Cancer Res, 2012. **72**(4): p. 876-86.
54. Dumitru, C.A., et al., *Neutrophils and granulocytic myeloid-derived suppressor cells: immunophenotyping, cell biology and clinical relevance in human oncology.* Cancer Immunol Immunother, 2012. **61**(8): p. 1155-67.
55. Pruenster, M., et al., *S100A8/A9: From basic science to clinical application.* Pharmacol Ther, 2016. **167**: p. 120-131.
56. Opal, S.M., et al., *Effect of eritoran, an antagonist of MD2-TLR4, on mortality in patients with severe sepsis: the ACCESS randomized trial.* JAMA, 2013. **309**(11): p. 1154-62.
57. Deguchi, A., et al., *Eritoran inhibits S100A8-mediated TLR4/MD-2 activation and tumor growth by changing the immune microenvironment.* Oncogene, 2016. **35**(11): p. 1445-56.

국문 초록

서론: 유방암의 면역 미세환경은 호르몬 수용체 발현이나 종양의 진행 단계에 따라 다양한 모습을 보인다. 종양 면역을 대상으로 하는 면역치료제의 효과가 입증됨으로서 유방암 면역에 대한 연구의 중요성은 날로 커지고 있다. 골수유래 면역억제세포는 종양 면역에 중요한 기능을 담당하고 있으나 그 표현형이 복잡하기 때문에 인체 조직에서 연구가 어려운 분야이다. 이 세포들은 면역과 관련된 기전 뿐만 아니라 면역과 관련되지 않은 기전을 통하여서도 다양하게 암의 진행을 촉진시킨다.

방법: 포괄적인 면역 프로파일링을 이용하여 비지도 군집분석과 호르몬 수용체 발현에 따른 면역 관련 유전자들의 발현 차이를 평가하였다. 추가 분석을 위하여 유의미한 발현량 차이를 보이는 유전자로 나타난 골수유래 면역억제세포 관련 유전자를 선택하였다. 700명의 유방암 환자 조직으로 만들어진 조직 마이크로어레이에서 해당 단백질 발현의 차이를 확인하였다. 이 단백질 발현이 가지는 임상병리학적 중요성과 다른 종양 침윤 림프구 (CD4, CD8, FOXP3 양성 림프구), PD-L1 양성 면역세포와의 관계를 분석하였다.

결과: 면역 프로파일링 자료를 비지도 군집분석에서 확인된 '군집 2'와 다른 군집들의 비교 및 호르몬 수용체 발현에 따라서 분석한 결과 골수유래 면역억제세포 표지자로 알려진 S100A8이 가장 큰 발현량 차이를 보였다. 면역조직화학염색 결과 S100A8은 유방암 조직의 종양세포와 면역세포 모두에서 염색되었다. 특히 S100A8 양성 면역세포의 침윤은 나쁜 임상병리학적 특성, 나쁜 예후와 관련이 있었다. 이들은 유방암의 침윤 전 단계부터 존재하였고 CD4, CD8, FOXP3 양성 종양 침윤 림프구, PD-L1 양성 면역세포 침윤의 증가와 연관을 보였다. S100A8 양성 면역세포의 예후적 중요성은 호르몬 수용체 양성인 경우, PD-L1 양성 면역세포가 없는 경우, CD8, FOXP3 양성 림프구가 적은 경우에 더 두드러지게 나타났다. 다양한 면역조직화학검사 결과 S100A8 양성

면역세포는 대부분 CD33 양성, CD15 음성, CD163 양성 표현형을 보여 단핵구 계열 골수유래 면역억제세포에서 기원한 대식세포로 생각되었다.

결론: S100A8은 특정 면역 군집을 구분하는 중요한 단백이며 또한 호르몬 음성 유방암에서 증가하였다. 인간 유방암 조직에서 S100A8은 주로 단핵구 계열 골수유래 면역억제세포에서 기원한 대식세포에서 발현되며 침윤 전 단계부터 존재하여 유방암의 진행을 촉진하는 역할을 할 것으로 생각된다. S100A8 양성 면역세포는 CD4, CD8, FOXP3 양성 종양 침윤 림프구와 PD-L1 양성 면역세포의 증가와 연관이 있었으나 그 예후적 중요성은 면역성이 낮은 조건에서 더 두드러지게 나타났다.

주요어: S100A8, 침윤성 유방암, 골수유래 면역억제세포, 종양 면역 미세환경, 종양관련 대식세포

학번: 2018-22261